Research Report
Tacoma Pile Driving
Agreement T1461, Task 11

UNDERWATER NOISE REDUCTION OF MARINE PILE DRIVING USING A DOUBLE PILE

by

Per G. Reinhall[1] Tim Dardis[1] and Peter H. Dahl[2]

[1]Department of Mechanical Engineering
[2]Applied Physics Laboratory
University of Washington
Seattle, Washington 98105-6698

Washington State Transportation Center (TRAC-UW)
University of Washington, Box 354802
University District Building, Suite 535
1107 NE 45th Street
Seattle, Washington 98105-4631

Prepared for

The State of Washington
Department of Transportation
Lynn Peterson, Secretary

December 2015

Testing in Commencement Bay

TECHNICAL REPORT STANDARD TITLE PAGE

1. REPORT NO. WA-RD 849.1	2. GOVERNMENT ACCESSION NO.	3. RECIPIENT'S CATALOG NO.
4. TITLE AND SUBTITLE UNDERWATER REDUCTION OF MARINE PILE DRIVING USING A DOUBLE PILE		5. REPORT DATE December 2015 6. PERFORMING ORGANIZATION CODE
7. AUTHOR(S) Per G. Reinhall, Tim Dardis, Peter H. Dahl		8. PERFORMING ORGANIZATION REPORT NO.
9. PERFORMING ORGANIZATION NAME AND ADDRESS Washington State Transportation Center (TRAC) University of Washington, Box 354802 University District Building; 1107 NE 45th Street, Suite 535 Seattle, Washington 98105-4631		10. WORK UNIT NO. 11. CONTRACT OR GRANT NO. Agreement T1461, Task 11
12. SPONSORING AGENCY NAME AND ADDRESS Research Office Washington State Department of Transportation Transportation Building, MS 47372 Olympia, Washington 98504-7372 Rhonda Brooks, Project Manager, 360-705-7945		13. TYPE OF REPORT AND PERIOD COVERED Research Report 14. SPONSORING AGENCY CODE
15. SUPPLEMENTARY NOTES This study was conducted in cooperation with the U.S. Department of Transportation, Federal Highway Administration.		

16. ABSTRACT

Impact pile driving of steel piles in marine environments produces extremely high sound levels in the water. It has been shown that current pile driving noise attenuation techniques, such as bubble curtains and cofferdams, provide limited noise reduction because significant noise is transmitted through the sediment into the water. Similarly, the effectiveness of surrounding the pile in the water with a double walled steel tube was shown in an earlier WSDOT study to be limited. To address this problem, a double walled pile has been developed to decrease the total noise transmitted into the water. The double walled pile consists of two concentric tubes connected by a special driving shoe, with an air gap between the two tubes. The double walled pile is driven into the sediment by using traditional equipment to strike the inner tube only. The air gap between the inner and outer tube prevents the radial deformation wave produced by the pile hammer from interacting with the water and the sediment. This report discusses the design of the double wall pile and presents the results from finite element modeling of the pile, scaled prototype testing, and full-scale field testing in Commencement Bay, Puget Sound, Washington. The tests showed that the double walled piles reduce the peak sound pressure over 20 dB relative to single walled piles at a range of approximately 8 meters. They also showed that, in contrast, only a 3- to 6-dB reduction is obtained when a bubble curtain is used on a full-scale, single walled pile.

17. KEY WORDS Pile driving impact, acoustics, underwater noise, attenuation, propagation	18. DISTRIBUTION STATEMENT No restrictions. This document is available to the public through the National Technical Information Service, Springfield, VA 22616

19. SECURITY CLASSIF. (of this report) None	20. SECURITY CLASSIF. (of this page) None	21. NO. OF PAGES	22. PRICE

DISCLAIMER

The contents of this report reflect the views of the authors, who are responsible for the facts and the accuracy of the data presented herein. The contents do not necessarily reflect the official views or policies of the Washington State Department of Transportation or Federal Highway Administration. This report does not constitute a standard, specification, or regulation.

Table of Contents

LIST OF FIGURES

LIST OF TABLES

EXECUTIVE SUMMARY

Impact pile driving of steel piles in marine environments produces extremely high sound levels in the water. It has been shown that current pile driving noise attenuation techniques, such as bubble curtains and cofferdams, provide limited noise reduction because significant noise is transmitted through the sediment into the water. Similarly, the effectiveness of surrounding the pile in the water with a double walled steel tube was shown in an earlier Washington State Department of Transportation study [1] to be limited to approximately 10 dB because of the unconstrained propagation of Mach sound waves [1-3] directly from the sediment into the water.

To address this problem, a double walled pile has been developed to decrease the total noise transmitted into the water. The double walled pile consists of two concentric tubes connected by a special driving shoe, with an air gap between the two tubes. The double walled pile is driven into the sediment by using traditional equipment to strike the inner tube only. The air gap between the inner and outer tube prevents the radial deformation wave produced by the pile hammer from interacting with the water and the sediment. In one embodiment of the double pile design the inner tube can be removed and repeatedly reused.

This report discusses the design of the double wall pile and presents the results from finite element modeling of the pile, scaled prototype testing, and full-scale field testing in Commencement Bay, Puget Sound, Washington. The tests showed that the double walled piles reduce the peak sound pressure over 20 dB relative to single walled piles at a range of approximately 8 m. They also showed that, in contrast, only a 3- to 6-dB reduction is obtained when a bubble curtain is used on a full-scale, single walled pile.

1 INTRODUCTION

Impact pile driving of steel piles in marine environments produces extremely high sound levels in the water. It has been shown that not only are current noise attenuation techniques costly to use, but they also provide limited noise reduction [4-7]. This is because the noise from pile driving is transmitted through the sediment into the water [1-3]. In Reinhall and Dahl [1-3] we showed, using modeling and field data, that the primary source of underwater sound from an impact driven pile is radial expansion of the pile as the compression wave propagates down the pile after each strike. The radial expansion is coupled to the compression wave through the Poisson's ratio of steel. As discussed in Reinhall and Dahl [1-3], the supersonic (with respect to the water) radial expansion wave produces an acoustic field in the shape of an axisymmetric cone, or Mach cone. We showed in Reinhall and Dahl [1-3] that the ability of any sound shield that surrounds the pile only in the water (such as a bubble curtain or a surrounding double wall engagement) to attenuate the sound in the water is limited by the fact that an upward moving Mach sound wave is produced in the sediment and is transmitted into the water. To improve the performance of bubble curtains and other noise shields in the water, the noise emanating from the sediment into the water must also be attenuated. Figure 1 illustrates how sound from the seabed leaks out from the sediment, limiting the effect of the surrounding bubble curtain.

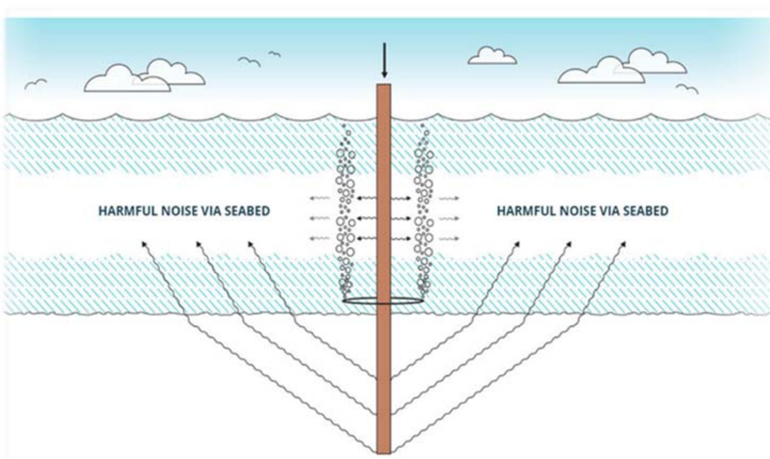

Figure 1: Illustration of how sound from the seabed is transmitted unhindered by a sound shield surrounding the pile in the water, e.g., a bubble curtain.

2 BACKGROUND

2.1 Marine Pile Driving

Steel pipe piles are a common aspect of deep foundations. Concrete piles are also often used. Each has its advantages and disadvantages. In terms of underwater noise produced during impact driving, it is known that for the same diameter, a concrete pile will produce less noise [8]. The reason is twofold: a) concrete material has a lower Poisson's ratio than steel, and b) concrete piles are typically solid in cross-section. These two attributes result in lower radial deformation of the pile per unit of axial deformation.

This is shown in Figure 2, and further described in Reinhall and Dahl [1-3]. The hammer strike produces a compression wave in the pile and an associated radial displacement motion because of the effect of Poisson's ratio of the pile material.

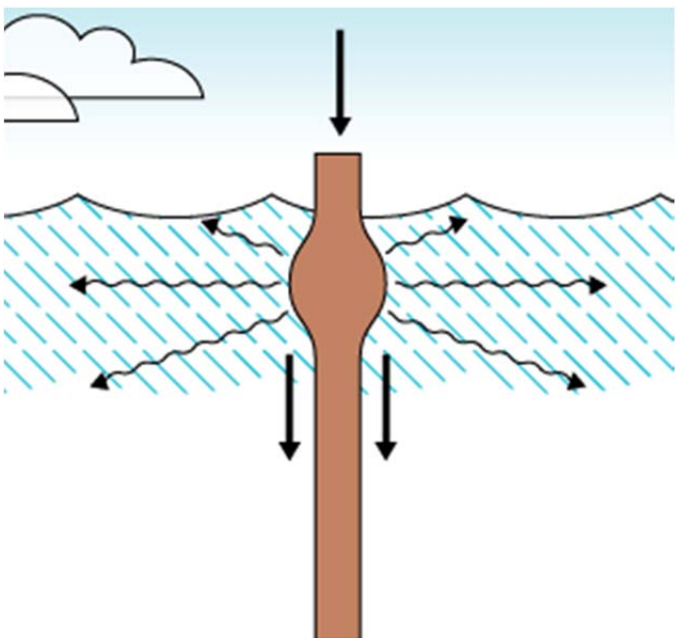

Figure 2: Illustration of the radial displacement wave after a hammer strike.

The speed of the downward traveling radial displacement wave in the pile is higher than the speed of sound in the water. This produces an acoustic field in the shape of an axisymmetric cone, or Mach cone. Essential properties of the Mach cone were verified by modeling and measurements in Reinhall and Dahl [1-3]. There are, of course, additional contributions to the underwater noise field associated with pile vibrations. However, the field associated with this Mach cone is the one that clearly dominates peak pressure, as can be seen in Figure 3.

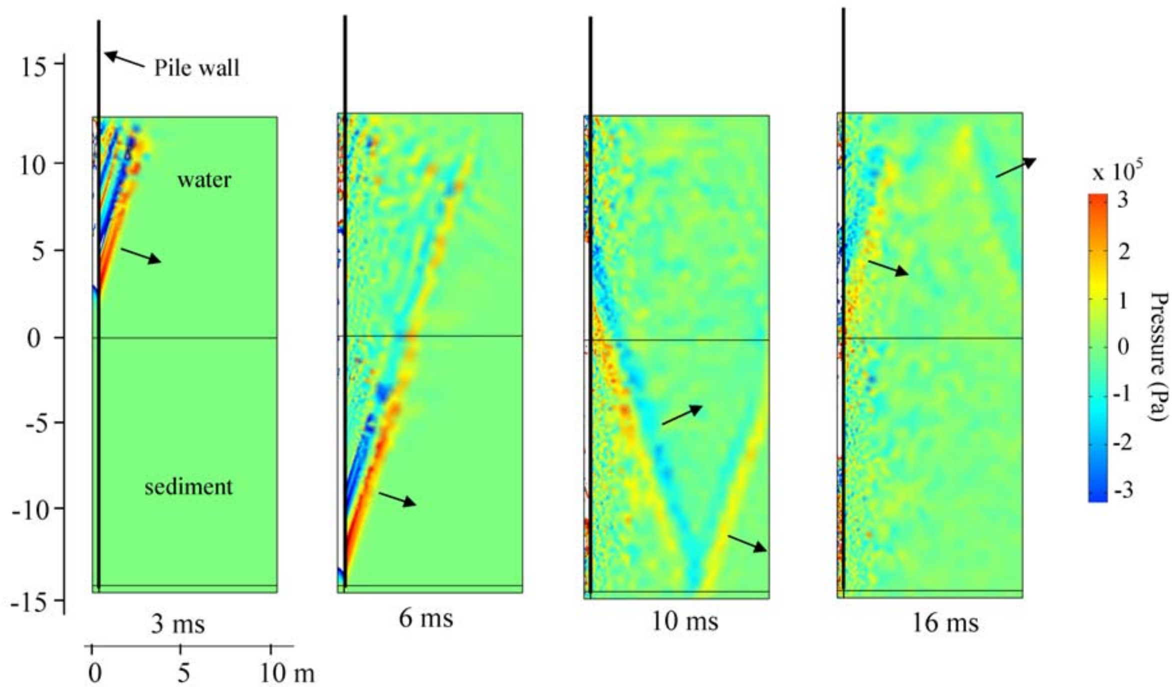

Figure 3: Acoustic pressure surface plots showing the acoustic radiation from the pile after 3, 6, 10, and 16 ms after impact by a pile hammer.

As the deformation wave reaches the bottom end of the pile (approximately 6 ms after impact for a 100-ft pile), it is reflected upwards, since there is an impedance mismatch between the pile and the sediment. This reflected wave in turn produces an upward moving Mach cone. The sound field associated with this upward moving cone propagates up through the sediment and penetrates into the water. For a detailed description, refer to the previous WSDOT report [1] and our papers [2,3].

2.2 Underwater Noise and the Environment

Underwater noise created by impact pile driving can reach peak sounds level in excess of 210 dB [8]. These levels have deleterious effects on local fauna [9-13]. Because of the critical state of many animal populations, U.S. Fish and Wildlife Service and several departments within the National Oceanic and Atmospheric Administration, including the Office of Protected Resources and the National Marine Fisheries Service, have instituted national guidelines regulating underwater noise generation through strict permitting procedures. These procedures are explained in detail on the Washington State Department of Transportation and Office of Protected Resources websites [14,15]. Underwater noise thresholds are shown in Table 1.

Table 1: Underwater noise thresholds for Endangered Species Act and Marine Mammal Protection Act listed species in the Pacific Northwest

	Injury Threshold	Non-Auditory Injury Threshold	Disturbance Threshold
MARBLED MURRELETS (Diving Birds)	202 dB $_{SEL}$	208 dB $_{SEL}$	N/A
CETACEANS (Whales, Porpoises)	180 dB $_{RMS}$	N/A	160 dB $_{RMS}$
PINNIPEDS (Seals, Sea Lions)	190 dB $_{RMS}$	N/A	160 dB $_{RMS}$
FISH ($\geq$ 2 Grams)	187 dB $_{SEL}$	N/A	150 dB $_{RMS}$
FISH (All Sizes)	206 dB $_{Peak}$		

2.3 Noise Attenuation Using a Sound Shield in the Water

As mentioned above, under typical conditions noise from pile driving is not effectively reduced by simply surrounding the pile with a sound shield in the water, such as a bubble curtain or a double walled shroud. Figure 4 shows an axisymmetric surface plot of the total acoustic pressure at 5, 8, 11, 13 and 17 ms after impact of a 100-ft long, 30-in steel pile **with a perfect acoustic shield**. It can be seen that the sound shield removes all the noise produced by the part of the pile that is submerged in the water. A Mach cone is not produced until the compression wave and the associated radial bulge reach the sediment and leave the surrounding shield. The radial deformation in the pile and the apex of the

Mach cone, which is now contained within the sediment only, reach the bottom end of the pile approximately 6 ms after impact for this particular pile length. As in the case for the untreated pile, an upward moving Mach cone is produced after the first reflection of the structural wave. Approximately 8 ms after impact, the upward moving structural wave and the apex of the Mach cone reach the shield and the water-sediment interface. The wave front is again propagating inside the acoustic shield, and the propagation of the Mach cone is ceased. However, the upward moving Mach wave that was produced in the sediment reaches the water-sediment after 8 ms and continues to propagate up into the water.

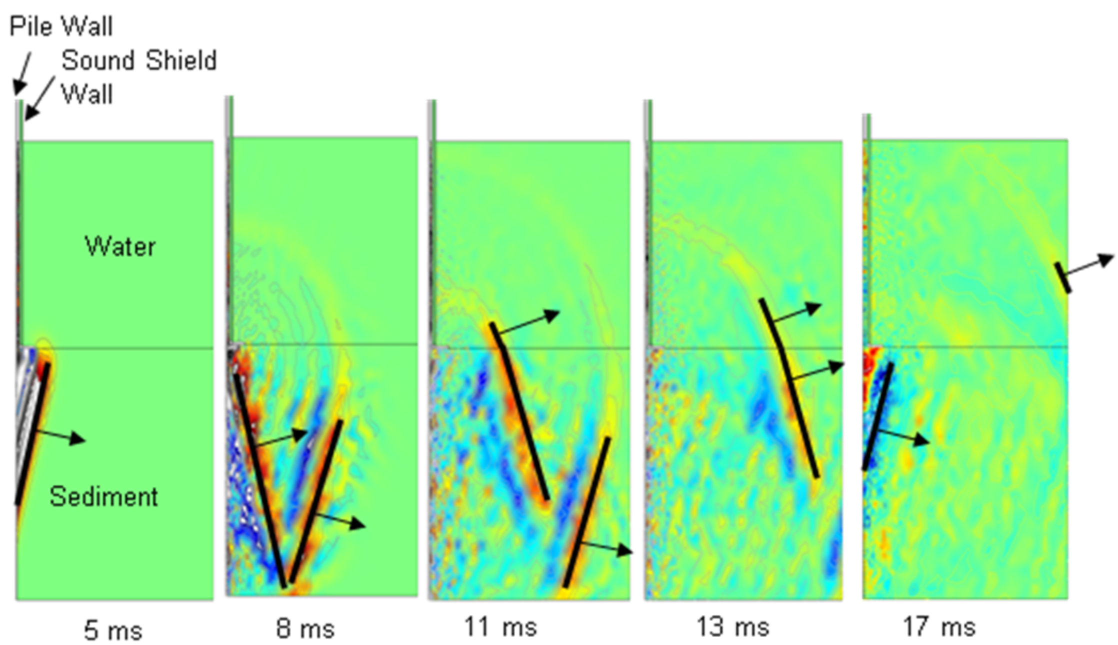

Figure 4: Acoustic pressure surface plots showing the acoustic radiation from the pile with the acoustic shield at 5, 8, 11, 13 and 17 ms after impact by a pile hammer.

The modeling results were confirmed by a full-scale field test (see [2] and the WSDOT Report [1]). The difference between the peak pressure from an untreated pile and sound shield covered pile was measured to be approximately 10 dB at an approximate range of 10 meters. This and other research showed that without containing the sediment borne noise, steel pipe piles cannot be installed without exceeding the established underwater noise thresholds.

3 DOUBLE WALL PILE

Figure 5 shows the double pile as described in Dardis and Reinhall [16-19]. This double pile concept was developed to combat the fact that a significant portion of the noise from marine pile driving is transmitted through the sediment into the water. The pile consists of two concentric pipes separated by an air gap and joined by a driving shoe designed to provide a flexible and water tight connection between the inner and outer pipes. The double pile assembly is driven into the sediment by striking the inner pile **only**. The air gap between the inner and outer pile prevents the radial deformation wave that is produced in the inner pile by the pile hammer strike from interacting with the water. The outside pile is effectively decoupled from the noise emanating from the inner pile.

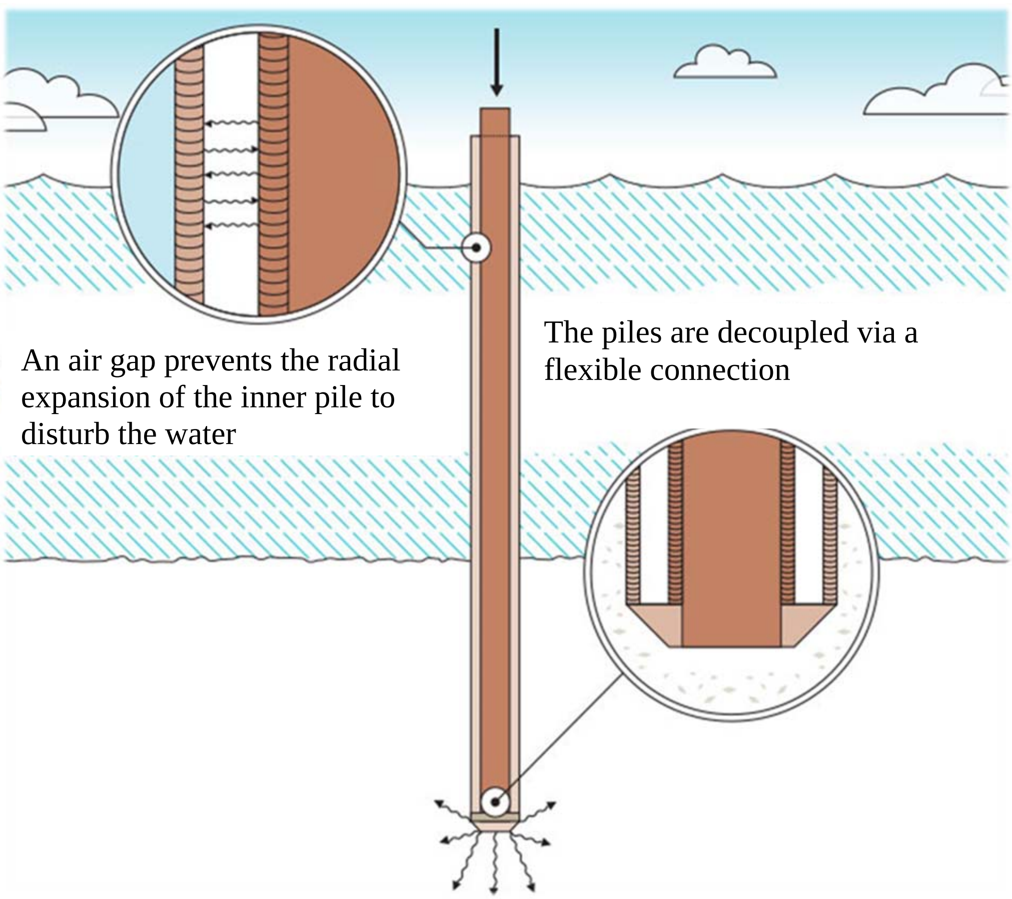

Figure 5: Schematic of the double wall pile

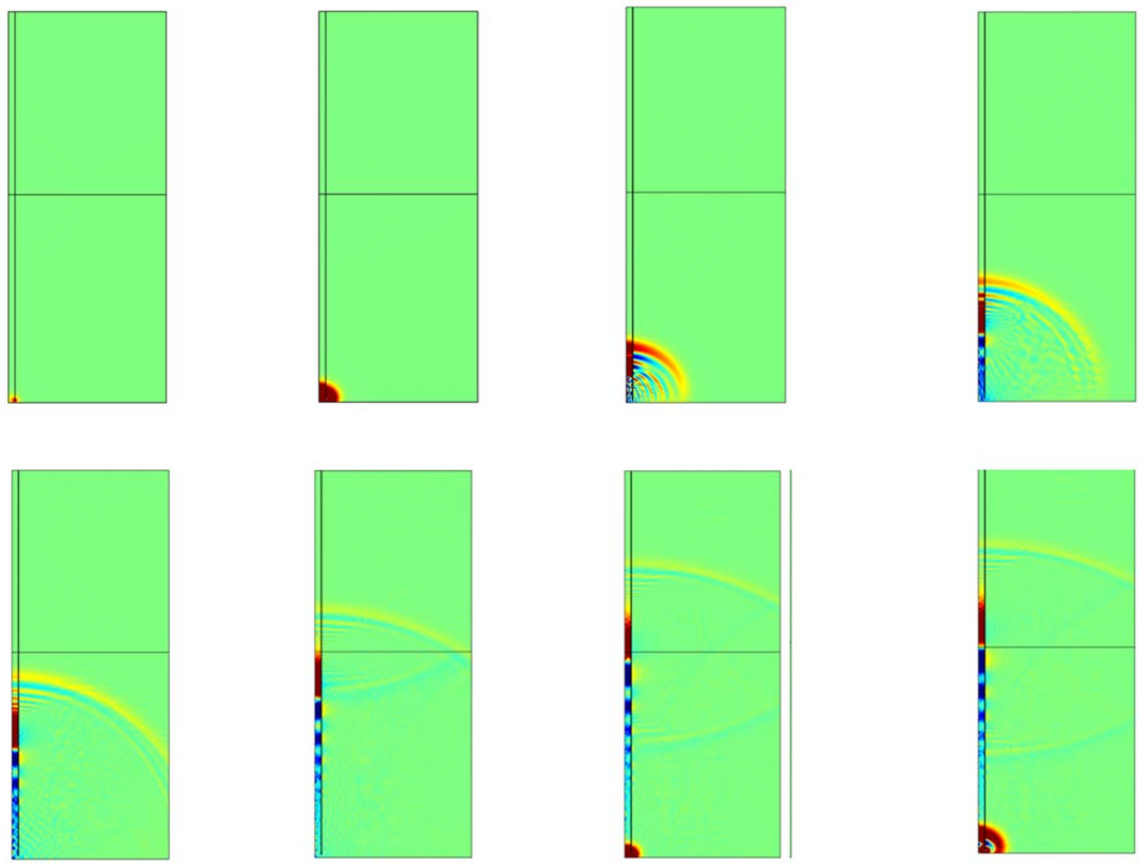

Figure 6: Initial double pile finite element modelling

Finite element modelling was used to develop and fine-tune the double pile configuration. Figure 6 contains axisymmetric contour plots produced by the analysis. These plots show where the sound is initiated and how the sound propagates away from the pile. Clearly the noise generation at the pile wall has been eliminated. The remaining noise is created as the pile toe advances into the soil substrate. The upper left plot is a snapshot in time right when the pile compression wave reaches the pile toe and begins to be reflected back up the inner pile. The lower right plot shows the pile when the inner pile wave has travelled back to the pile toe.

Another key feature of this design is that traditional pile installation methods are maintained. It was determined during our early concept exploration that preservation of the industry’s capital equipment would be essential if the design would be used in wide scale practice.

3.1 Subscale Field Test

To explore the double pile concept, 3-inch-diameter aluminium piles and 3-inch-diameter steel piles were constructed. The small scale was chosen to minimize cost and maximize handling.

Initial testing was completed in air. The research team soon discovered that in air, noise was challenging to record because of the low pile noise to ambient noise ratio. The next series of experiments was conducted by using a hydrophone with the pile toe submerged in a large container filled with water.

The latter method produced promising results. These results encouraged the research team to create a dedicated subscale testing facility in a local body of water. Six inch diameter piles were designed and built. These piles were used to validate the results discovered during the testing of 3-inch-diameter piles. Figure 7 shows more detailed finite element modelling of the design. Additional information can be found in Dardis and Reinhall [16,18].

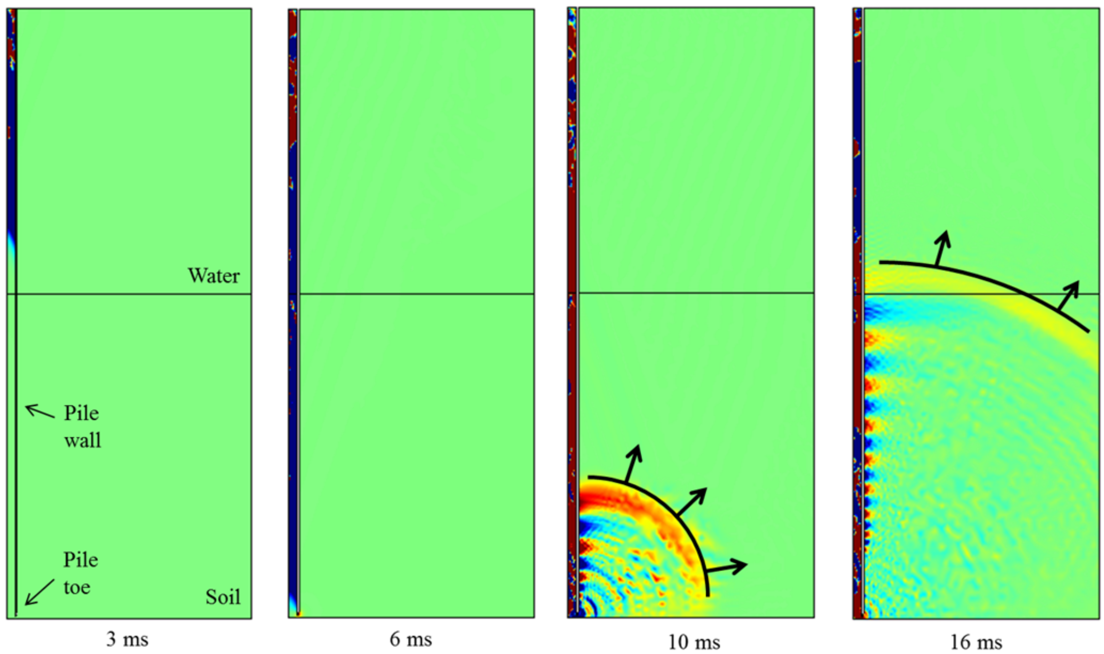

Figure 7: Finite element modelling of the 6-inch double pile

The two piles were held concentrically to one another by placing a foam spacer in the annulus between the two pipes. This prevented any pile to pile contact during driving.

3.1.1 Design/Build of Sub-Scale Piles

To validate the finite modelling, subscale piles were constructed for testing. The piles consisted of a single wall control pile with pile shoe and a double wall test pile with a shoe designed to provide a flexible coupling and a watertight seal. The control pile and the outer pile of the double wall had an outside diameter of 6 5/8 inch and a wall thickness of 0.280 inch. The outside diameter of the inner pile was 5 9/16 inch with a wall thickness of 0.258 inch.

3.1.2 Sub-Scale Pile Installation

An impact hammer was constructed adjacent to a dock in a local lake. The hammer consisted of a mass and a guide rod. The mass was elevated above the pile with a hand operated winch. The guide rod was used to ensure that the mass struck the top of the pile in a consistent manner. Figure 8 shows the pile being readied for impact.

Figure 8: A subscale pile being prepared for testing

Acoustic monitoring was done with a single Aquarian H2a hydrophone. The hydrophone signal was recorded and processed with Audacity and MATLAB software, respectively. Both were loaded onto a typical laptop computer. The hydrophone was located 10 m from the test pile. The drop height of the mass was set so that the single pile signal was near saturation.

3.1.3 Test Results

Testing matched computational models, and the double pile provided a signal 20 dB lower than the single wall pile. This is shown in figures 9 and 10 and documented in Dardis and Reinhall [16].

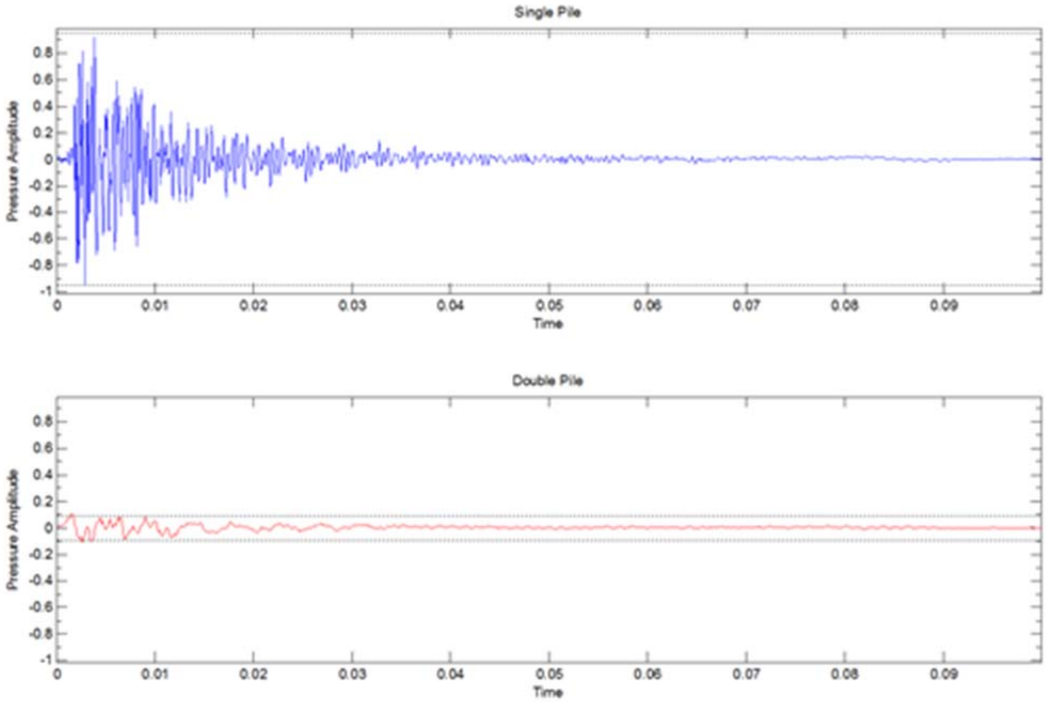

Figure 9: p(t) plots comparing a single wall pile (top) and a double wall pile (bottom)

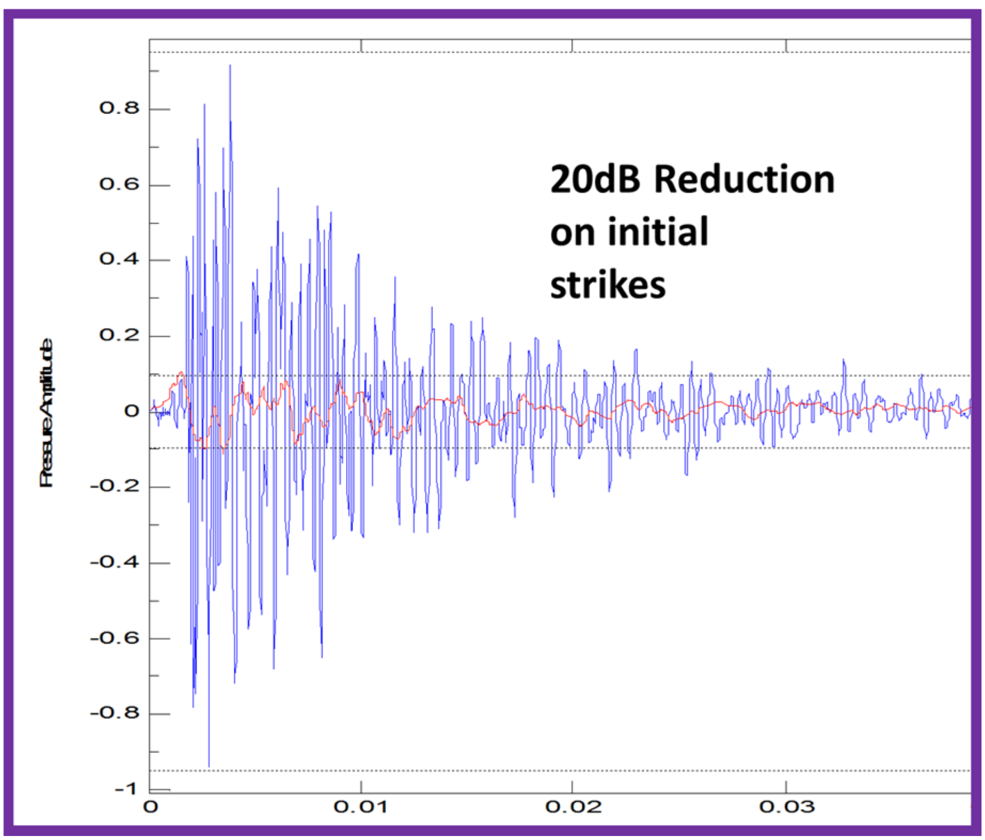

Figure 10: p(t) pile signals overlaid and magnified

3.2 Full-Scale Field Test

After the success of the sub-scale test, modeling and development of double walled and mandrel piles were completed to support a full-scale field test.

Figure 11: Delmag D46 Impact hammer being set to the control pile

The acoustic radiation from a regular single wall pile and the double wall pile was investigated by using dynamic axisymmetric finite element modeling using an implicit finite element code (Comsol Multiphysics). The model was made to be consistent with the piles used in our full-scale test in Commencement Bay in Puget Sound, Washington. The outer diameter of the single wall control pile was 30 inch with a wall thickness of 0.75 inch. Figure 11 shows the installation of this pile. The outer and inner piles in the double wall pile had an outer diameter of 30 inch and 24 inch, respectively. The wall thickness of the outer pile was 0.75 inch. The wall thickness of the inner pile was 0.625 inch. The length of the piles was 80 ft.

A domain of water and sediment of 10 m in radius was included in the finite element model. Reflections from the boundaries of the truncated domain were effectively prevented by using non-reflecting boundary conditions.

The pressure, p(t), resulting from the impact between the hammer weight and the pile was approximated by $p(t) = 2.1\ 10^8 \exp(-t/\tau)$ Pa, where t is time after impact in seconds and the time constant τ is equal to 0.004s [1,2]. The water and air sound speeds, c_w, c_a, were set to 1485 m/s and 340 m/s, respectively, and the sediment was modelled as a fluid with sound speed, c_s, equal to 1625 m/s.

Figure 12 shows the sound field around a regular single wall pile and our double wall pile for different times after hammer strike. It can be seen that high intensity Mach sound waves created by the deformation wave in the single pile are not present in the double pile. The only significant sound source of the double pile is the pile shoe. This sound cannot be removed from the system because the pile toe must move in order for the pile to advance in the soil. This movement creates noise. The benefit of a localized noise source is that the sound waves decay more rapidly with distance travelled.

Because of the absence of high intensity Mach waves, our model yielded a reduction of the peak pressure in the water in excess of 20 dB in comparison to the regular pile.

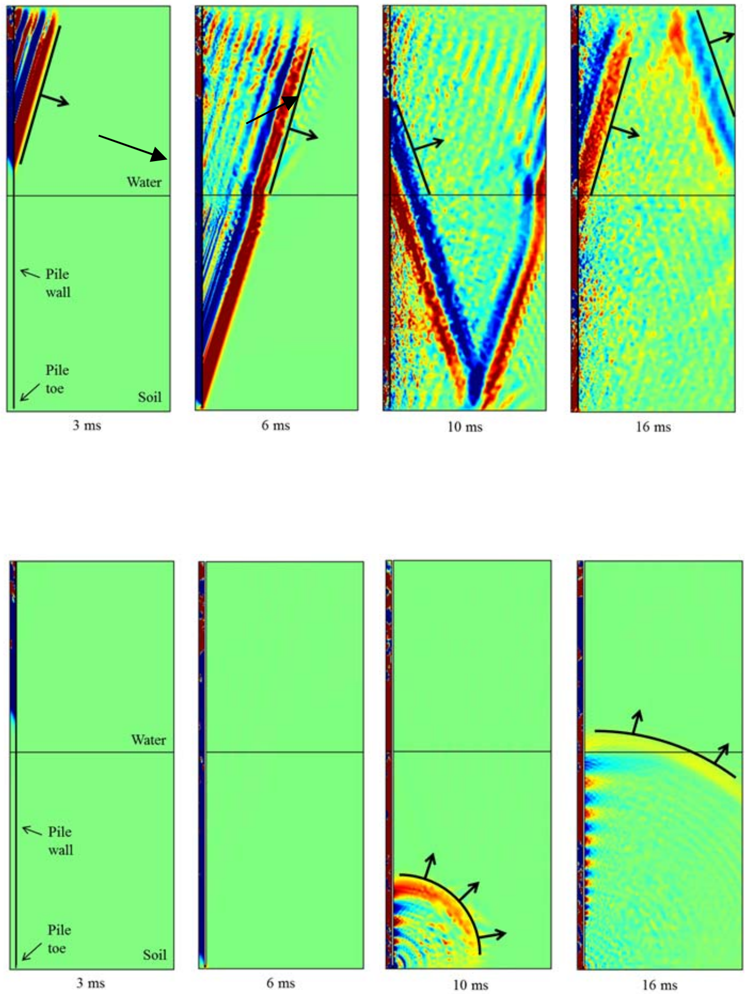

Figure 12: Acoustic pressure surface plots showing the acoustic radiation from the single pile (top) and the double pile (bottom) at 3 ms, 6 ms, 10 ms, and 16 ms after impact by a pile hammer.

3.2.1 Design for Minimum Cost Solution

The double pile solution can be realized in three different forms: Double Pile, Filled Double Pile, and Mandrel Double Pile. These are simplistically shown in Figure 13. Briefly stated, the advantages of each configuration are as follows:

<u>Double Pile</u>

- Simple
- Fast installation

<u>Filled Double Pile</u>

- Fast installation
- Higher strength/stiffness

Mandrel Pile

- Reusable inner pile
- Single wall construction

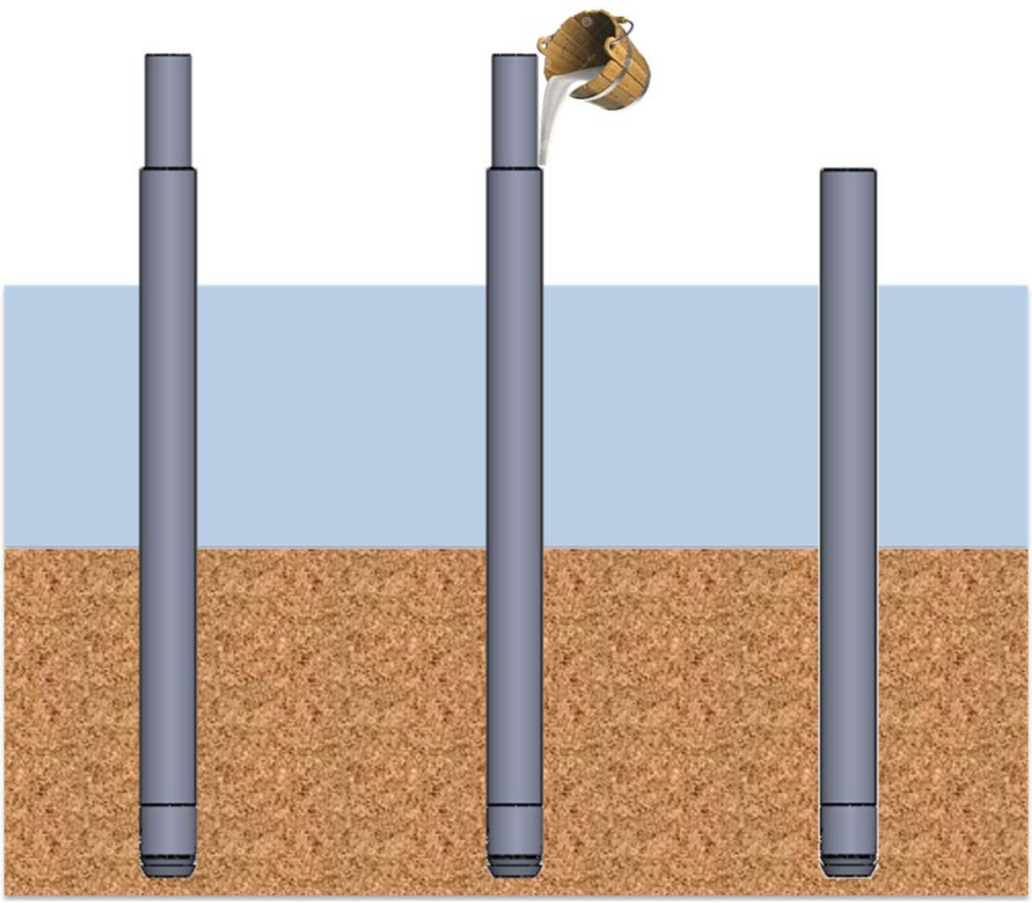

Figure 13: Double pile (left), filled double pile (center), mandrel double pile (right)

3.2.2 Design/Build of Full-Scale Piles

As described above, sub-scale and full-scale test piles were developed. Each of the completed piles consists of similar components: a shoe that helps to attenuate sound through the bottom substrate; a stem that affixes the shoe to two short sections of pipe (inner and outer) to facilitate welding to full length pipes; spacers to maintain separation between the inner and outer pipes; and welding of the stem to the full length pipes to form the complete double walled or Mandrel piles. Each of these components and the sequence of building the piles are described below.

3.2.2.1 Shoe

The design of the shoe for the double pile and the mandrel double pile incorporates as many common parts as possible. The assembly consists of a combination of machined steel, rolled pipe, and rubber parts. The inner shell parts were welded together to create an assembly. Similarly, the outer shell parts were welded together to create an assembly. The two shell assemblies were then mated with the rubber parts, which served as seals, spacers, and springs. Last, the shoe chisel was welded to the inner shell, creating a complete shoe assembly [20].

Figure 14 shows the completed shoe before being attached to the pipe.

Figure 14: Complete double pile shoe

3.2.2.2 Stem

The pile shoe was then welded to short sections of pipe to create a ‘stem’ (see Figure 15). The double pile shoe was attached to two sections of pipe, while the mandrel double pile was attached to only the outer section of pipe. The mandrel end was welded to the end of a section of pipe to form the ‘stem’ of the mandrel. The alignment between the pile shoe and the pipe is critical. To ensure this, an alignment jig was designed and used during fabrication of the stem.

Figure 15: Double pile stem as delivered to Orion Marine

3.2.2.3 Complete Pile

Orion Marine was contracted to complete the final fabrication of the piles. The pile stems were delivered to Orion Marine in 40-foot sections. During this fabrication Orion Marine attached pile spacers, as shown in Figure 16. These spacers provided insurance that there would be no pile to pile contact during driving.

Figure 16: Installation of pile spacers

A traditional pile splice bed was used to ensure pile straightness during the welding process. A straightness requirement of 0.1 percent was used.

The mandrel was also delivered to Orion Marine as a 40-foot section and had the same external dimensions as the inner pile of the double pile. Because the mandrel was designed to be removed from the system after the outer pile has been driven, the end of the mandrel was equipped with a reinforced toe that also served as a sealing surface to prevent water intrusion. Figure 17 shows the mandrel. The mandrel was also equipped with skids to facilitate installation. Figure 18 shows the complete piles ready to be installed.

Figure 17: Mandrel before and after pile installation

Figure 18: Full-scale double pile and mandrel double piles before installation

3.2.3 Test Preparation

This section will briefly describe the full-scale test site (location, considerations for choosing the site and site characteristics) and acoustic monitoring planned for the test.

3.2.3.1 Test Location and Geotechnical Considerations

The test was located along the northeast shore of Commencement Bay in Tacoma, Washington, as indicated by Figure 19.

Figure 19: Commencement Bay test site

This location was chosen because it was not a site for other construction activities (allowing for clearer acoustic monitoring); it had a limited depth to the bearing soil layer (allowing for relatively short test pile length); and it provided a water depth of approximately 10 m at the test piles (allowing for uninterrupted noise transmission). Figure 20 shows the tidal level as a function of time during the days of testing and demonstrates sufficient water depth during the test activities. Figure 21 provides an overview of the site-specific bathymetry. In addition, the site was chosen to represent soft substrate conditions, which are prevalent throughout the region. Boring log data indicated extremely soft material to 26 feet and till from 26 to 46 feet. Additional testing in significant denser glacial tills will be conducted in Puget Sound at the Vashon Island ferry terminal in November, 2015.

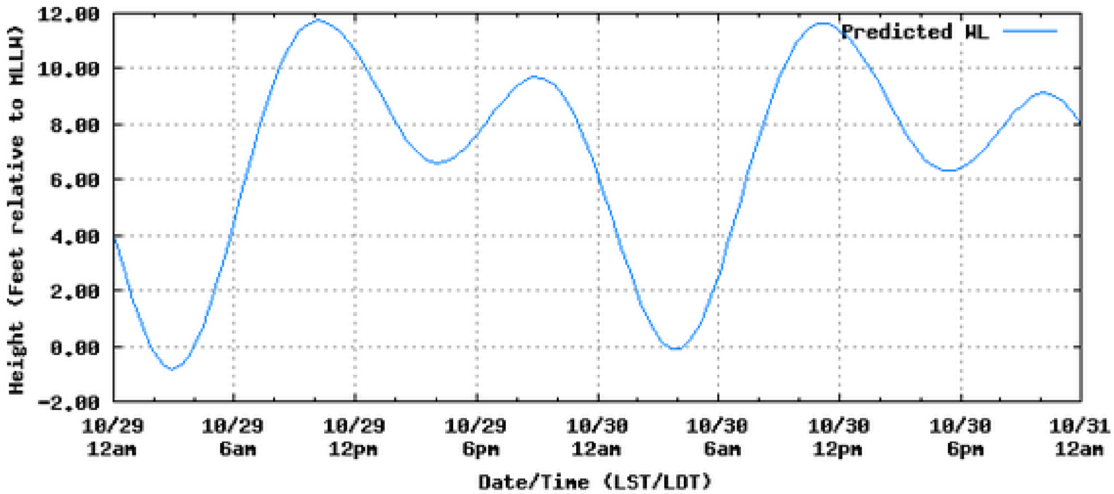

Figure 20: Tidal level on the date of the test

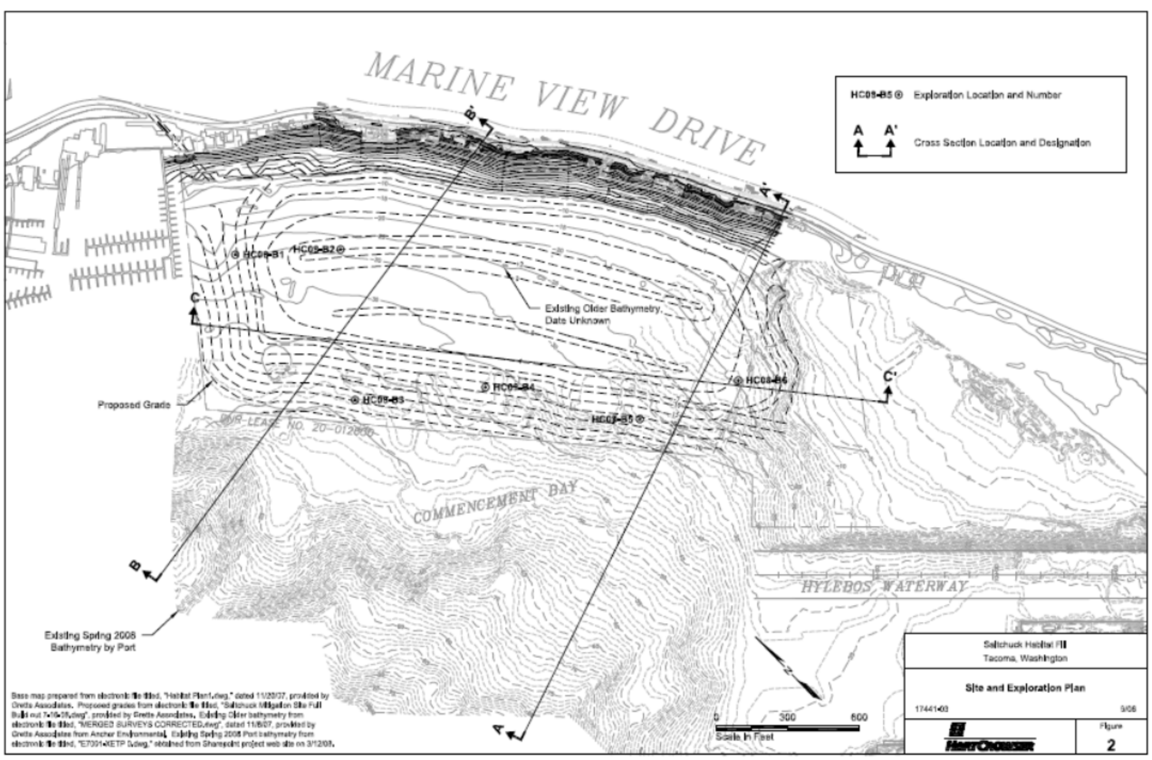

Figure 21: Bathymetry at the test site.

3.2.3.2 Acoustic Monitoring Plan

A previous report from the University of Washington, Applied Physics Lab, is found in the Appendix. This report provides a detailed summary of the acoustic monitoring plan and the results from the test. Figure 22 provides an overview of the location of the vertical line array and the individual hydrophones used in the monitoring. Figures 23 and 24 show areal views of the actual monitoring locations relative to the barge.

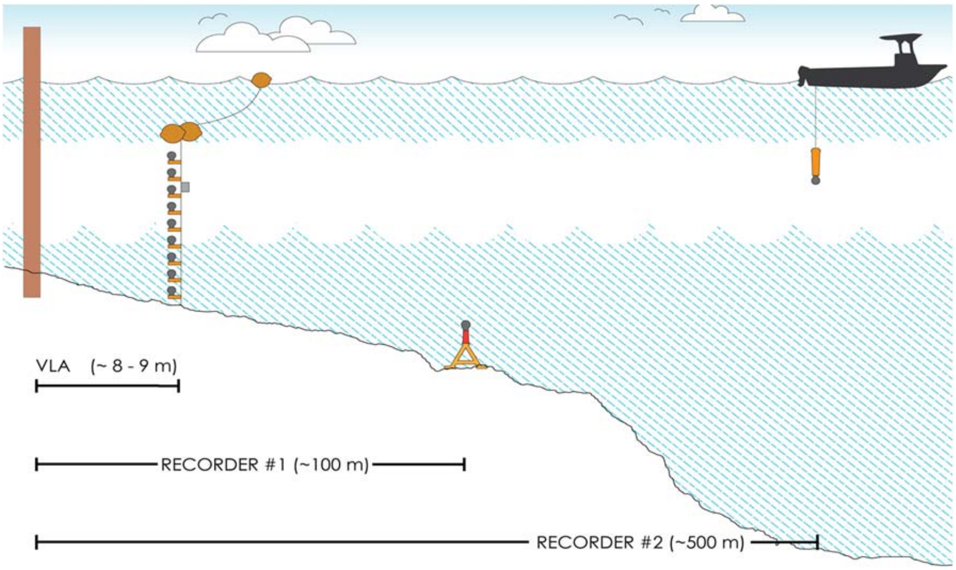

Figure 22: Locations of the hydrophones

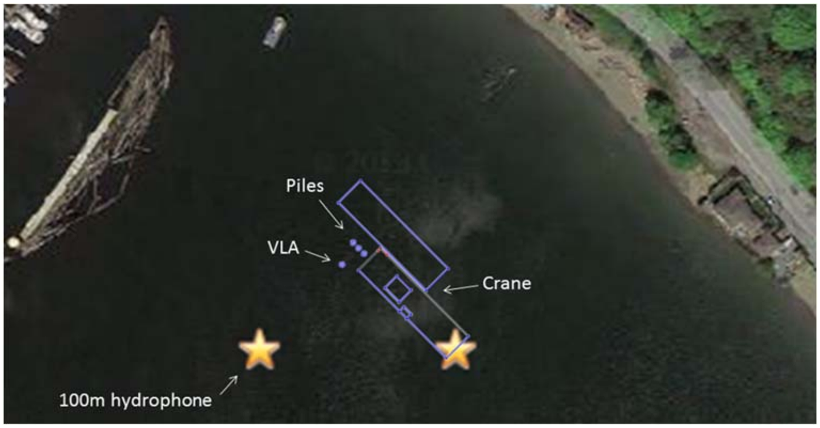

Figure 23: Placement of the near-field hydrophones

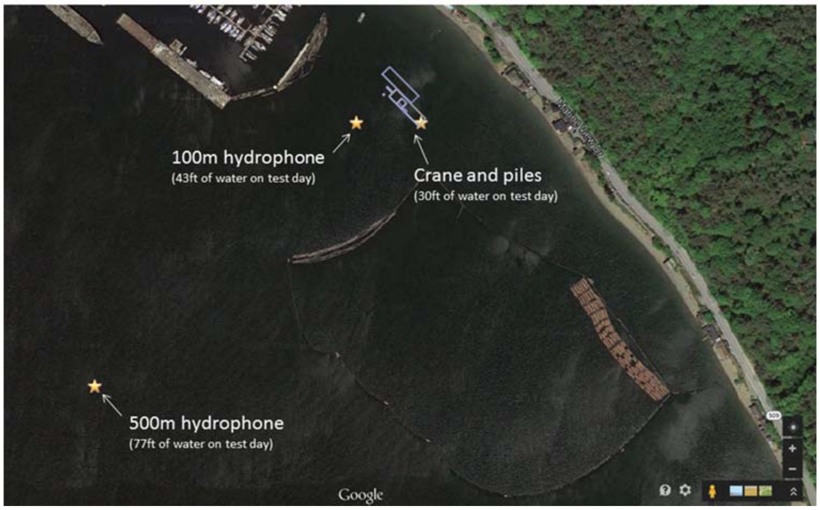

Figure 24: Placement of the far-field hydrophones

3.2.4 Full-Scale Pile Installation

The piles were installed by using a standard D46 hammer without the use of special equipment. Figures 25 and 26 depict the lofting and installation of the piles. Figure 27 shows the double pile and the control pile fully installed. The top end of the piles were driven to a few feet above the water level. No bearing capacity was specified due to the soft sediment and limited length of the piles (80 ft).

Figure 25: Day of testing

Figure 26: Lofting of the double pile

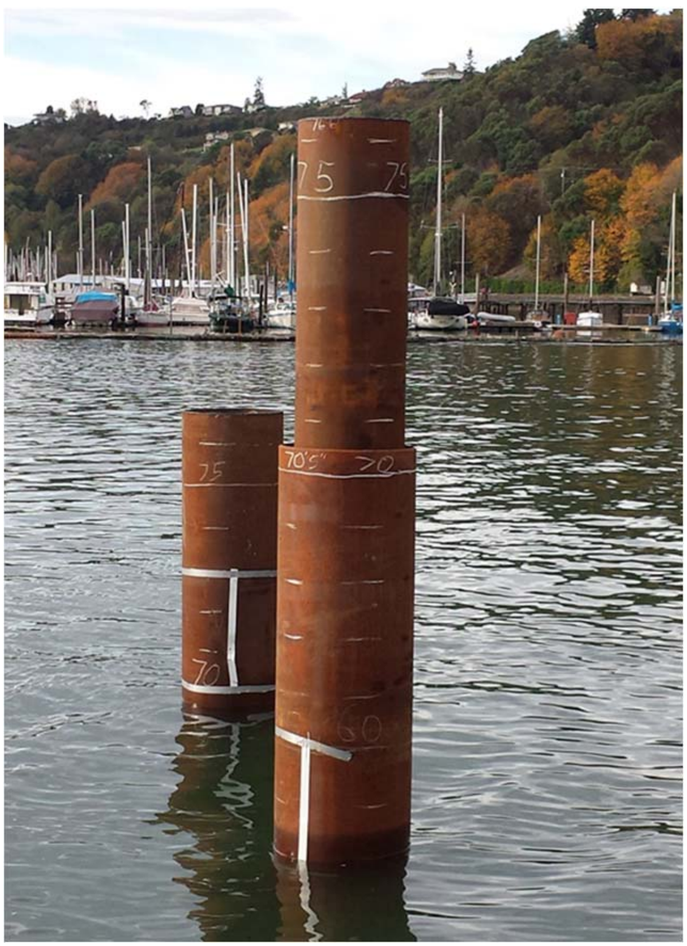

Figure 27: Control pile and double pile after driving

3.2.5 Test Results

During the installation of the piles, monitoring of the underwater noise was ongoing. The following figures provide a summary of the monitoring results from the full-scale field test.

Figure 28 shows a typical pressure recording of the sound from the control pile (red) and from the double wall pile (black) taken with the second lowest situated hydrophones in the VLA. A dramatic decrease in the peak pressure can be seen.

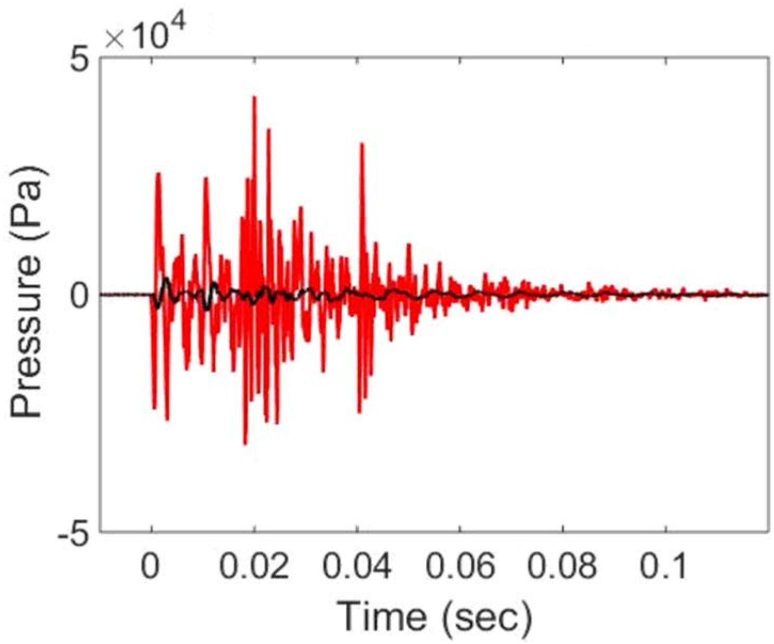

Figure 28: A typical pressure recording after a hammer strike measured at an 8-m distance from the control pile (red) and the double pile (black).

Figure 29 summarizes the results for underwater noise reduction in terms of SEL, RMS, and Peak pressure for the double wall test pile and the mandrel test pile relative to the control pile. It can be seen that the attenuation levels were significantly higher with the double wall pile and the mandrel pile over a conventional bubble curtain. A reduction of the peak pressure in excess of 21 dB was observed with the double and the mandrel piles, while the reduction using a bubble curtain was measured to be approximately only 6 dB. The RMS and SEL levels showed > 19 dB and >17 dB reduction, respectively.

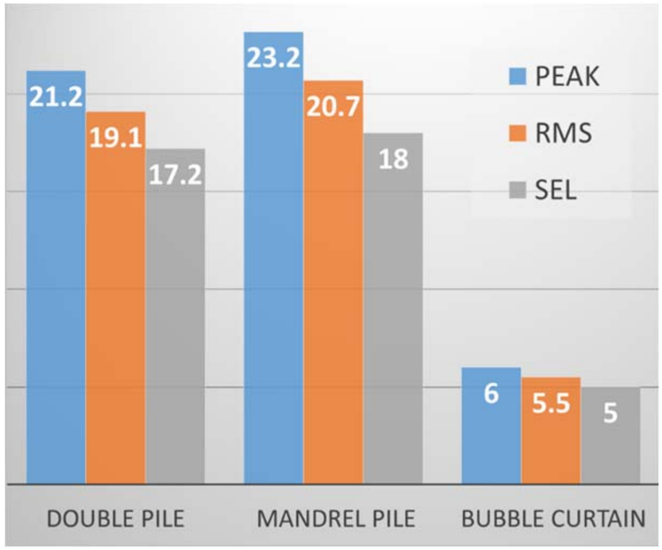

Figure 29: Summary of the results of the acoustic measurements in dB

In comparison to existing biological thresholds that currently inform the regulations of underwater noise related to the disturbance and potential injury to sensitive species, the noise generated by the impact installation of the test piles largely fell below them.

Table 2 summarizes the measured noise levels at a range of approximately 8 meters in comparison to established biological thresholds. The black numbers indicate measured sounds levels that are below most thresholds and therefore avoid associated impacts to sensitive species. The red numbers indicate sound levels that are above one or more of the established thresholds (orange shading). It can be seen that the double wall and the mandrel pile only exceed the RMS disturbance threshold for cetacean/pinniped species. It can also be seen that the sound levels associated with the control are high enough to exceed all thresholds established for fish, cetacean injury, cetacean/pinniped disturbance, and pinniped injury.

Table 2: Table of measured values at 8m vs. thresholds

	DOUBLE WALL PILE	FISH	CETACEAN INJURY	CETACEAN / PINNIPED DISTURBANCE	PINNIPED INJURY	MURRELET INJURY	MURRELET NON-AUDITORY
PEAK	190 dB	206 dB	-	-	-	-	-
$RMS_{90\%}$	179 dB	-	180 dB	160 dB	190 dB	-	-
CSEL	166 dB	187/183 dB	-	-	-	202 dB	208 dB
	MANDREL	**FISH**	**CETACEAN INJURY**	**CETACEAN / PINNIPED DISTURBANCE**	**PINNIPED INJURY**	**MURRELET INJURY**	**MURRELET NON-AUDITORY**
PEAK	188 dB	206 dB	-	-	-	-	-
$RMS_{90\%}$	177 dB	-	180 dB	160 dB	190 dB	-	-
CSEL	165 dB	187/183 dB	-	-	-	202 dB	208 dB
	CONTROL	**FISH**	**CETACEAN INJURY**	**CETACEAN / PINNIPED DISTURBANCE**	**PINNIPED INJURY**	**MURRELET INJURY**	**MURRELET NON-AUDITORY**
PEAK	211 dB	206 dB	-	-	-	-	-
$RMS_{90\%}$	198 dB	-	180 dB	160 dB	190 dB	-	-
CSEL	183 dB	187/183 dB	-	-	-	202 dB	208 dB

Another advantage associated with the noise reduction provided by the double pile is a decrease in the size of the required monitoring zone to avoid harassment and injury to sensitive marine wildlife. The noise levels for the double pile at 8 m were below National Marine Fisheries Service injury thresholds for all species and below disturbance thresholds for all but cetaceans and pinnipeds. The area potentially ensonified to a sound level exceeding the disturbance thresholds, i.e., the monitoring zone for disturbance for those species, shrunk dramatically, as shown in Figure 30. Whereas the approximate radius of the monitoring zone for the control pile (red) was 2.8 km and that for the double wall piles (yellow) was only 150 m. This smaller zone presents a concomitant reduction in the probability that sensitive species will occur inside this smaller area, which in turn means less risk of potential disturbance to marine species and less potential for work stoppage.

Figure 30: Comparison of monitoring zones.

4 ACKNOWLEDGMENTS

This research was supported by the Washington State Department of Transportation (WSDOT) with additional support from the Federal Highway Administration. The authors would like to thank Rhonda Brooks, Marion Carey, and Jim Laughlin at WSDOT for their strong support throughout this research.

In addition the authors are indebted to Bill Rehe for assistance with permitting. Bill interfaced with the following agencies/organizations, allowing the full-scale test to occur: US Army Corps of Engineers, City of Tacoma, Port of Tacoma, Washington State Department of Natural Resources, Washington Department of Fish and Wildlife, US Fish and Wildlife Service, and NOAA Fisheries.

5 REFERENCES

1. Reinhall, P.G. and P.H. Dahl. 2011. An Investigation of Underwater Sound Propagation from Pile Driving. Research report prepared for Washington Department of Transportation. Olympia, Washington. 45 pp.

2. Reinhall, P. G. and P.H. Dahl. 2011. Underwater Mach wave radiation and pile driving: theory and observation. Journal of the Acoustical Society of America. February, 2011. 25 pp.

3. Dahl, PH., and Reinhall, PG. "Observations and Parabolic Wave Modeling of Underwater Pile Driving Impact Noise." The Journal of the Acoustical Society of America 129 (2011): 2461.

4. Petrie, F.S. 2005. Washington State Ferries' Experience with Bubble Curtains: Purpose, Hardware, and Use. Presentation for 2005 Summer Meeting/Conference of the Transportation Research Board ADC40 (A1F04) Noise & Vibration Committee.

5. Koschinski, S. and K. Luedemann. 2013. Development of Noise Mitigation for Offshore Wind Farm Construction. Prepared for the Federal Agency for Nature Conservation (Bundesamt für Naturschutz, BfN). Original report published July 2011, English translation published February 2013. 102 pp.

6. CALTRANS (California Department of Transportation). 2009. Technical Guidance for Assessment and Mitigation of the Hydroacoustic Effects of Pile Driving on Fish_Prepared by ICF Jones & Stokes and Illingworth and Rodkin. Sacramento, CA. February 2009. 298 pp.

7. Applied Physical Sciences. 2010. Mitigation of Underwater Pile Driving Noise During Offshore Construction: Final Report. Prepared for Department of the Interior, Minerals Management Service Engineering & Research Branch. Herndon, VA. 104 pp.

8. WSDOT. 2015. Biological Assessment Preparation – Advanced Training Manual. *Table 7-12, Unmitigated Sound Pressure Levels Associated with Pile Types* in WSDOT 2015. Olympia, Washington. Available at: http://www.wsdot.wa.gov/NR/rdonlyres/448B609A-A84E-4670-811B-9BC68AAD3000/0/BA_ManualChapter7.pdf

9. Teachout E. 2006. Evaluating and minimizing the effects of impact pile driving on the marbled murrelet (Brachyramphus marmoratus), a threatened seabird. IN: Proceedings of the 2005 International Conference on Ecology and Transportation, Eds. Irwin CL, Garrett P, McDermott KP. Center for Transportation and the Environment, North Carolina State University, Raleigh, NC: p. 32. (Abstract)

10. Carlson, T.J., S.L. Sargeant, G.E. Johnson. 2004. Plan for Pile-driving Research. Technical report prepared for Washington Department of Transportation. Olympia, Washington. 106 pp.

11. Southall B.L., A.E. Bowles, W.T. Ellison, J.J. Finneran, R.L. Gentry, C.R. Greene Jr., D. Kastak, D.R. Ketten, J.H. Miller, P.E. Nachtigall, J. Richardson, J.A.Thomas, and P.L. Tyack. Marine Mammal Noise Exposure Criteria: Initial Scientific Recommendations. Aquatic Mammals, Volume 33, Number 4, 2007. 121 pp.

12. Marine Mammal Commission Report to Congress, Marine Mammals and Noise: A sound approach to research and management, March 2007

13. Halvorsen M.B., Casper B.M., Woodley C.M., Carlson T.J., Popper A.N. 2012. Threshold for Onset of Injury in Chinook Salmon from Exposure to Impulsive Pile Driving Sounds. PLoS ONE 7(6): e38968. doi:10.1371/journal.pone.0038968. 11pp.

14. WSDOT Website for noise thresholds: http://www.wsdot.wa.gov/Environment/Biology/BA/BAguidance.htm#MarineMammals

15. NOAA website for Office of Protected Resources: http://www.nmfs.noaa.gov/pr/

16. Dardis JT and Reinhall PG, “New Methods in Impact Pile Driving Noise Attenuation”, Proceedings of UA2014, June, 2014

17. Dardis JT and Reinhall PG, “New Pile for Reduced Underwater Noise” Proceedings of 40th Annual Conference on Deep Foundations, Oct, 2015

18. Dardis JT and Reinhall PG, “New Offshore Pile for Reduced Acoustic Emissions – Results from Full Scale Testing”, Proceeding of ICSV22, July, 2015

19. Reinhall PG and Dardis JT, “Promising New Method to Reduce Marine Pile Driving Noise” PileDriver, 2015 (2), pp 101-104

20. U.S. Patent 8,622,658, Reinhall and Dahl, Pile to Minimize Noise Transmission and Method of Pile Driving, 2014

6 APPENDIX

Measurement of Impact Pile Driving Noise from Prototype Piles in Commencement Bay, Tacoma, Washington

Measurement of Impact Pile Driving Noise from Prototype Piles in Commencement Bay, Tacoma, Washington

Peter H. Dahl, Per G. Reinhall, Tim Dardis, Jim Laughlin, Dave Marver, Alex Soleway and Dara Farrell

University of Washington, Seattle

Executive Summary

Underwater noise measurements for the purpose of evaluating the noise reduction performance of two new pile designs from the University of Washington were conducted on October 29-30, 2014 in Commencement Bay in cooperation with the Washington State Department of Transportation and Port of Tacoma.

Measurements of the underwater noise from impact pile driving were first made using a standard, 30-inch pile (October 29^{th}) followed by measurements on two reduced-noise pile designs both involving 30 inch piles; one a double-walled prototype (October 29^{th}) and the other double-walled mandrel prototype (October 30^{th}).

Measurements were made at a range of 8 to 8. 5 m from the piles using a 9-element vertical line array (VLA) and at two remote locations, at 122 m and 502 m (October 29^{th}) and at 135 m and 535 m (October 30^{th}). The underwater sound metrics used for comparison were the peak (absolute value) pressure (PEAK) in dB re 1 μPa, the root mean square pressure over time period covering 90% of pulse energy (RMS) in dB re 1 μPa, the Sound Exposure Level (SEL) in dB re 1 μPa^2-sec. Of these metrics, SEL is the most robust and noise reduction of approximately 18 dB is observed. Higher levels of reduction in the PEAK (21-23 dB) were observed at the VLA site but not at the distant sites. The reduction occurred over a broad frequency range (Appendix A) and was not frequency selective.

In terms of permitting, On October 29^{th} a total of 185 pile strikes were made. At the remote range of 122 m the cSEL was determined to be 183 dB re 1 μPa^2 sec, based on computation of the single SELs for all strikes (Appendix B). Based on the modeling the estimated range to the 187 dB cSEL isopleth was approximately 60 m. On October 30^{th}, there were a total of 70 strikes of much lower energy level (because unmitigated control pile was not used) and cSEL was estimated to be 184 dB re 1 μPa^2 sec at range of about 8 m, setting the 187 dB cSEL isopleth range to be less than 10 m.

I. Introduction

This report summarizes the results of underwater noise measurements for the purpose of evaluating the noise reduction performance of two new pile designs from the University of Washington as part of a research effort funded by the Washington State Department of Transportation and FHWA.

The Port of Tacoma has joined the research effort by identifying a test site in Commencement Bay (Fig. 1) for field testing and assisting with the permit process. Tests were conducted on October 29-30, 2014.

The tests are divided into three basic phases the first two conducted on October 29th and the third phase on October 30th:

(1) A standard 30-inch diameter steel pile as the control pile (CP). During the first part of this test an industry standard unconfined bubble curtain was cycled on and off to also measure the noise reduction efficiency of the bubble curtain.

(2) Test Pile 1: A 30-inch diameter steel double-walled prototype pile (DWP)

(3) Test Pile 2: A 30-inch diameter steel double-walled prototype mandrel pile (MP)

Additional details relating to the three phases are given in Sec. IV.

Figure 1. Vicinity map of Prototype Pile Test Project in Commencement Bay (blue shaded area).

II. Fixed Underwater Acoustic Measurement Locations and Geometry

Underwater acoustic measurements were made at three locations designed to measure underwater sound over an unobstructed propagation path between pile source and acoustic receiver. The first was a 9-element vertical line array (VLA) with hydrophone separation of 0.7 m. Hydrophone sensitivity was determined for each hydrophone and accounted for separately with average being -206 dB re 1 V/μPa. This system recorded with a single hydrophone sampling frequency of 62500 Hz. The position of the VLA with respect to the three test piles and barge complex is sketched in Fig. 2, photographs of the three piles made in shortly after testing on October 30th are shown in Figs. 3a and 3b. The relative position of the 9 hydrophones within the water column is shown in Fig. 4.

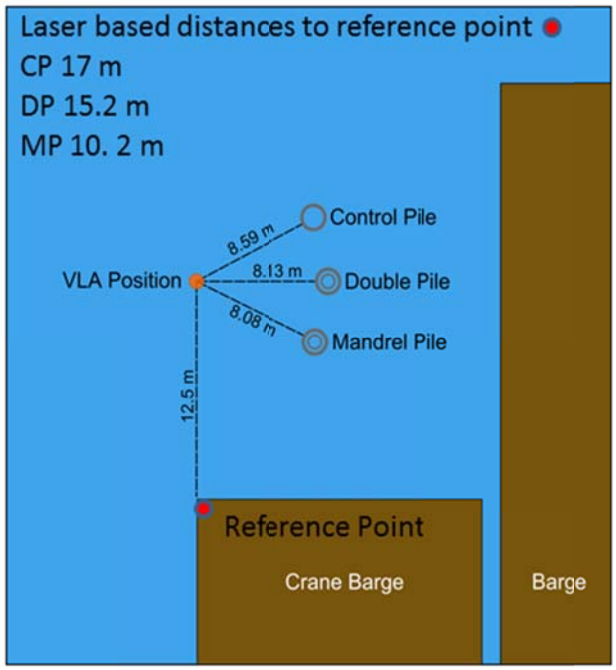

Figure 2. Position of the VLA with respect to the three test piles and barge complex.

Figure 3a. Photograph made on October 30th of the 3 piles shown in order of nearest to farthest: Mandrel Pile, Double Pile and Control Pile. Buoy marker on left shows approximate position of the VLA.

Figure 3b. Photograph made on October 30th of the 3 piles shown in order of nearest to farthest: Mandrel Pile, Double Pile and Control Pile. The VLA, now under tension is shown on the left while its range from the piles is measured.

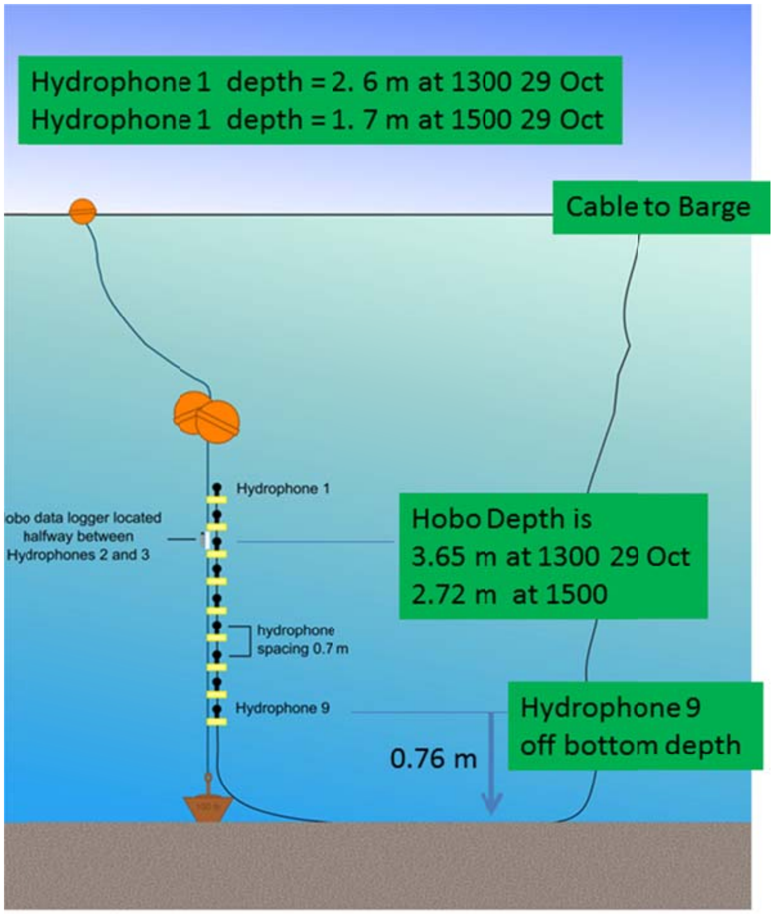

Figure 4. Position of the 9 hydrophones on the VLA with respect to depth. Note this relation changes according to tidal conditions. Tidal elevation 0900-0930, 30 October is similar to that at 1300 29 October.

The other two measurements were made at remote sites with ranges nominally at 100 m (Fig 5), and 500 m (Fig. 6) from the pile. Precise range depended on deployment conditions and for measurements on October 29th these ranges were 122 m and 502 m, respectively (applying to both Control Pile and Double Wall Pile). For the measurements on October 30th the ranges from the pile source were 135 m and 517 m, applying to the Mandrel Pile tests held that day.

At both remote sites measurements were made with an autonomous recording system (Loggerhead Systems) with hydrophone sensitivity equal to -206 dB re 1 V/μPa, sampling frequency equal to 50000 Hz. The closer (~ 100 m) system was deployed 1 m off the bottom mounted on the tripod as shown in Fig. 7, and the farther (~500 m) system was deployed over-the-side of the work vessel operated by *Citizens for Healthy Bay* at depth 10 m, while the vessel was anchored on site.

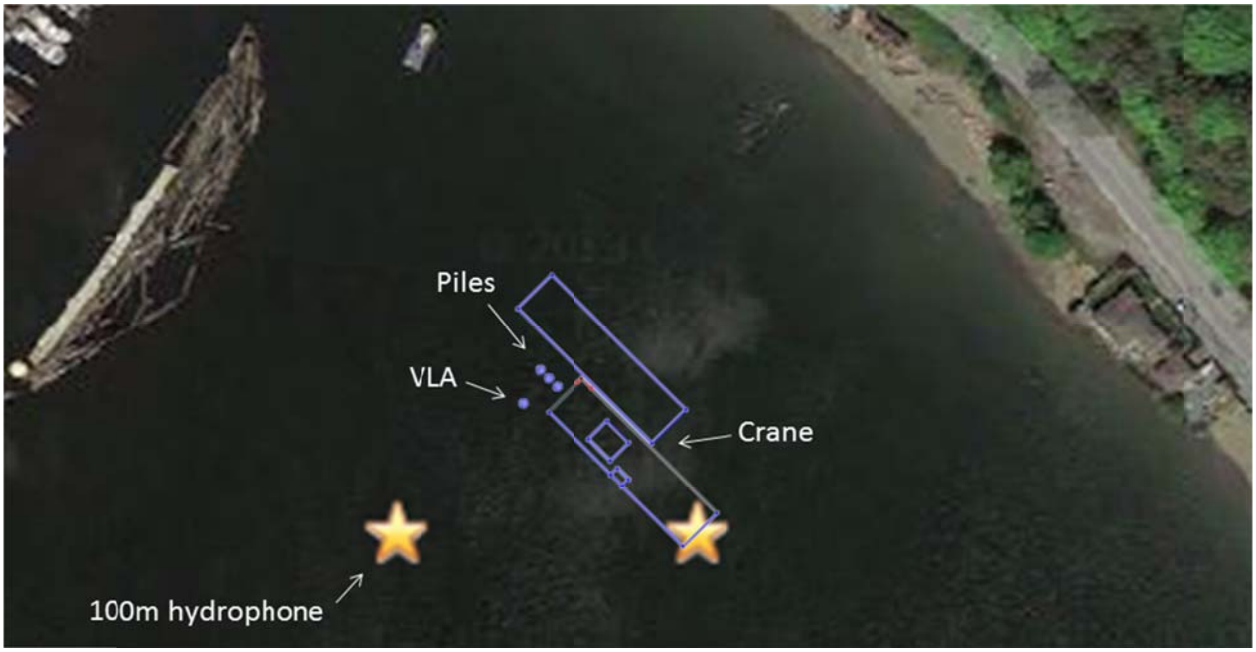

Figure 5. Notional position of the 100 m hydrophone with respect to the pile sources (see text for exact deployment range from piles.)

Figure 6. Notional position of the 500 m hydrophone with respect to the pile sources (see text for exact range from piles.)

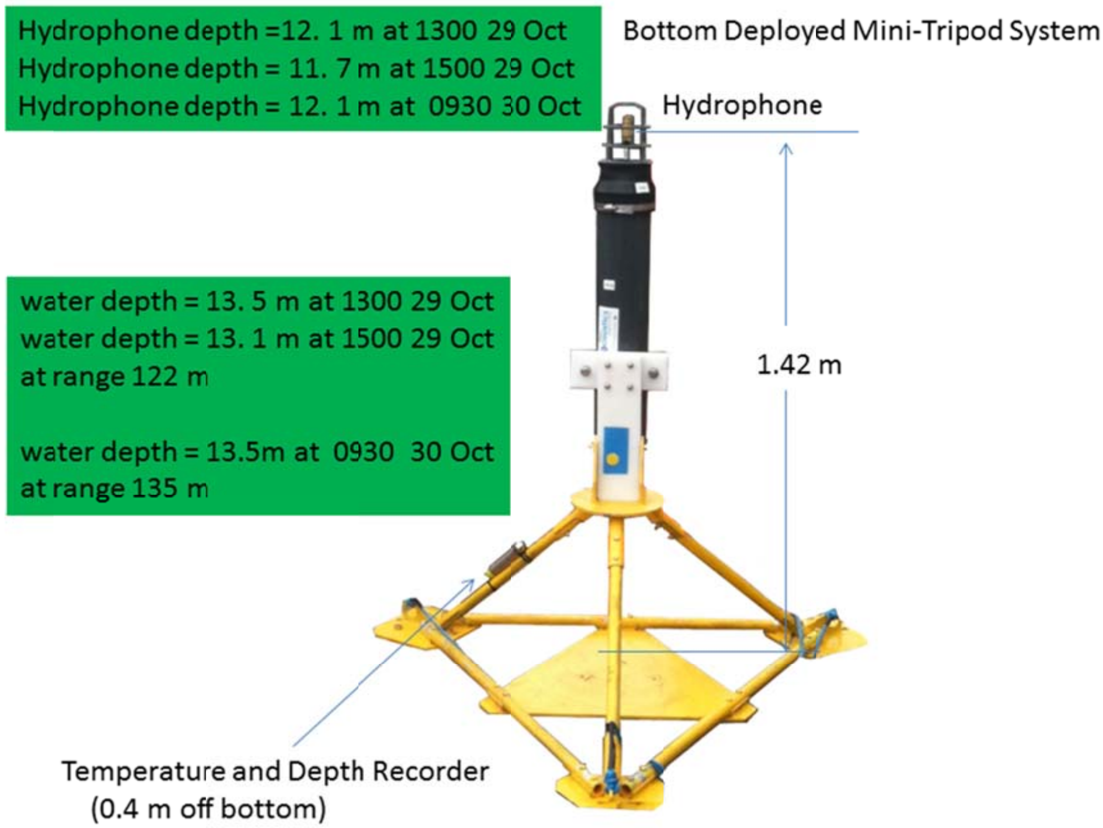

Figure 7. System deployed at notional 100 m range (see text for exact range from piles). Depths for the three key measurements are shown.

A 4th measurement location was used to obtain real-time estimates of underwater sound levels. At this stage of the report, we are forgoing interpretation of measurements from this location because of ambiguities relating to the sound path between pile source and acoustic receiver as shown in Figure 8. This path would have necessarily been under the barge would differ depending on pile test. Furthermore the 3 ft. drop in water level between 1300 and 1500 on October 29th further complicates interpretation because a larger fraction of the water column is blocked.

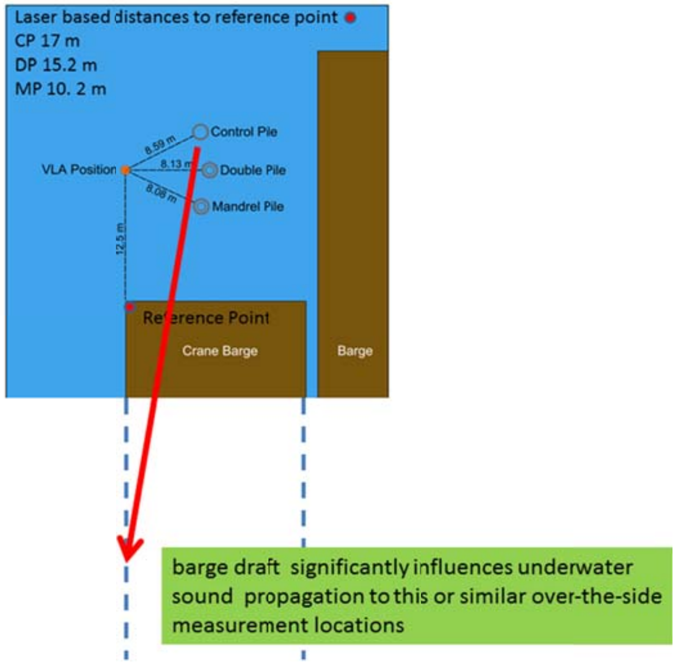

Figure 8. Showing potential issues relating to the underwater sound measurements taken over-the-side of the Crane Barge at the approximate location given by the red arrow head. The crane barge extends beyond the brown-colored area as shown by the dotted lines. The draft of the barge significantly influences underwater sound propagation in the direction of the red arrow. The influence depends on the particular pile under test.

III. General Environmental Conditions and Water Sound Speed

Conditions were generally ideal for the measurements as indicated by calm sea surface conditions shown in Figs. 9a and 9b. Water temperature measured at the bottom at the ~100 m site from the mini-tripod (Fig. 7), and on the VLA (Fig. 4) was 12^{o} C. A sound speed measuring device (YSI) was deployed from the *Citizens for Healthy Bay,* although this was unfortunately not recovered. However based on the temperature recordings and the salinity measurements made in Commencement Bay in 2013, we can estimate sound speed at 1490 m/s.

Figure 9. Photographs: Top (a) looking out from the site and, bottom (b) looking towards the pile source, both documenting the calm sea surface conditions in effect during the measurements.

IV. Basic sequence of Events

For measurement phase 1 on October 29th involving the control pile commencing approximately 12:18 pm, the basic sequence was as follows:

(i) A single "deadblow" defined as impacting the pile with weight of the hammer only, without additional energy supplied to the hammer.

(ii) A series of strikes during which the hammer fuel setting was changed from 1 to 4 (involving settings 1-2-3-4) and bubble curtain activation was either on or off. This series started about 10 min after the deadblow.

(iii) A final series of strikes during which hammer fuel setting was at maximum = 4. This series started about 24 min. after sequence (ii).

The complete record involving the control pile is shown in Fig. 10 (showing just channel 9 for simplicity) with exception of the single "deadblow" that occurred at approximately 12:20 pm. Data from sequence (ii) measured by channel 9 of the VLA is shown in upper figure and sequence (iii) in the lower figure (no strikes occurred within the 2-minute gap of the upper and lower figures.)

At the time of the writing of this draft report, the meta data required to establish the precise actions and their timing during sequence (ii) relating to changes in fuel settings and the bubble curtain, is not available. These changes modulated the peak pressure by approximately 10 dB (e.g., as shown in Fig. 11). Thus, for purposes of comparison between the control pile and the test pile we will only show results from the deadblow and sequence (iii).

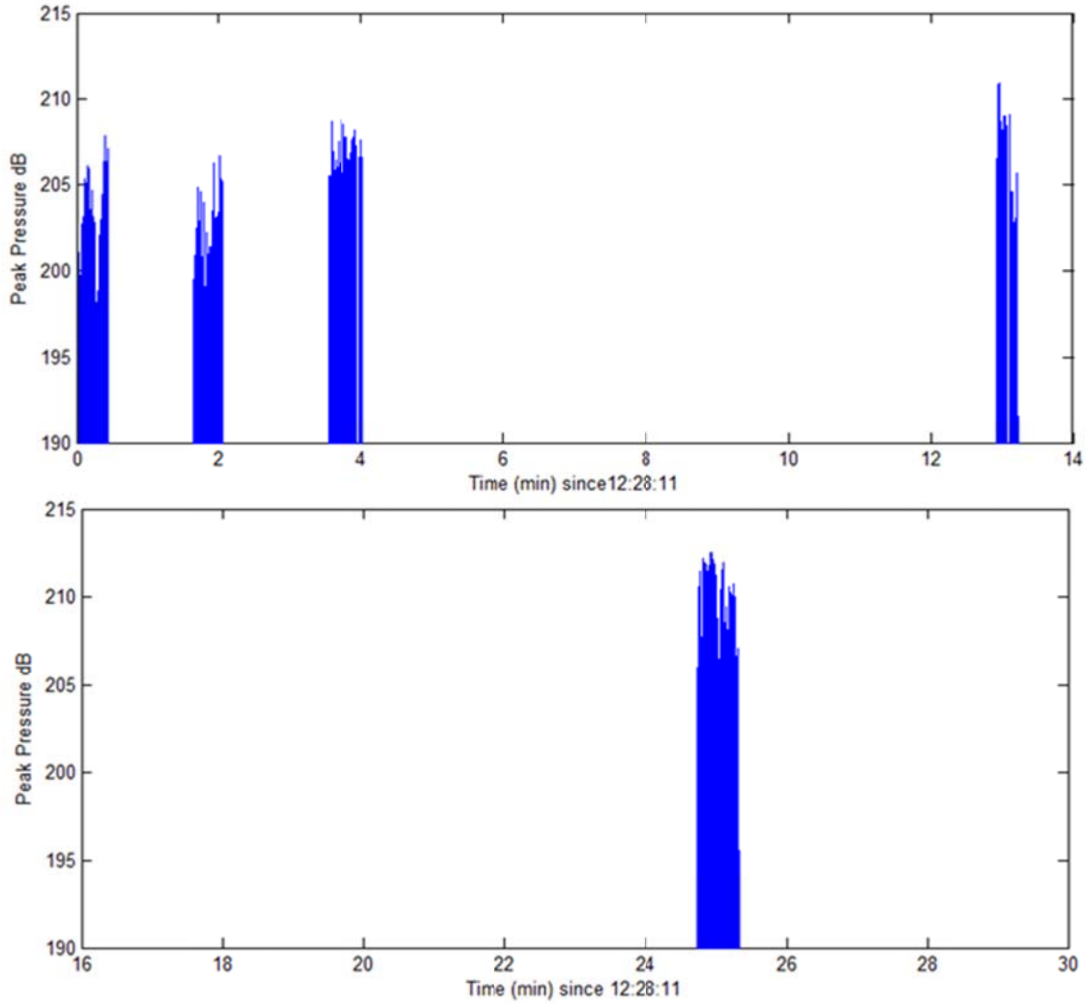

Figure 10. Pressure recording from channel 9 (lowest channel) of the VLA for series of hammer strikes made on the control pile on October 29th. Upper plot shows period during which the hammer fuel setting was changed and/or the bubble curtain was activated and deactivated. Lower plot shows final set of strikes during which the hammer fuel setting was held constant at setting = 4. Data are absolute pressure expressed in dB re 1 μPa.

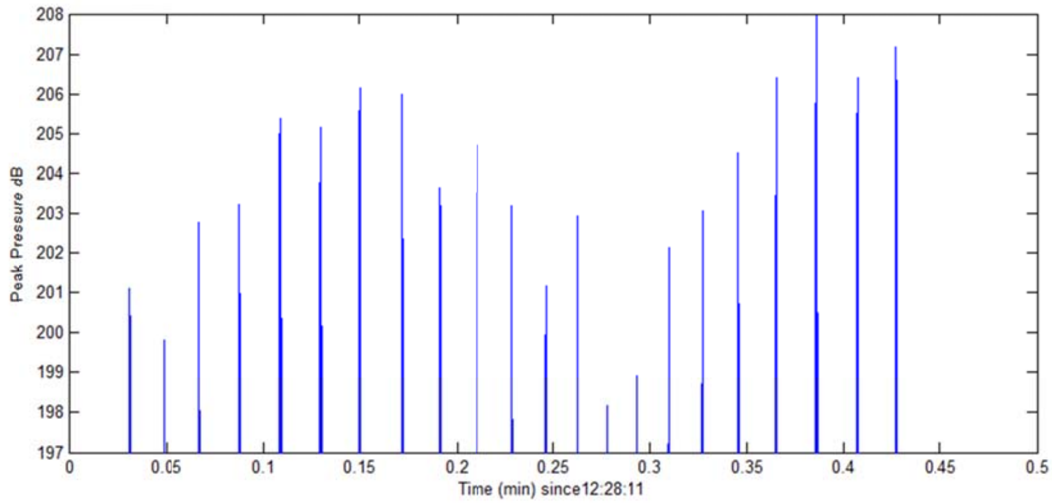

Figure 11. Expanded view of the first 30 sec from Fig. 10 (upper). NOTE: pressure is absolute pressure expressed in dB re 1 μPa, up to 10 dB changes are seen.

For measurement phase 2 on October 29th involving the double wall test pile commencing approximately 14:18 pm, the basic sequence was as follows:

(i) Two "deadblows" defined as impacting the pile with weight of the hammer only, without additional energy supplied to the hammer.

(ii) A series of strikes during which the hammer fuel setting was changed from 1 to 4 (involving settings 1-2-3-4). No bubble curtain was involved. This series started about 3 min after the deadblow.

(iii) A final series of strikes during which hammer fuel setting was at maximum = 4. This series constituted the last portion of series of strikes that started with sequence (ii)

The complete record involving the double wall test pile is shown in Fig. 12. Starting at approximately minute 4 (on the time scale of the figure) fuel settings were changed in an unknown manner and duration causing the modulation shown in yellow shade. The blue shade denotes the period where fuel setting was definitively set to, and held at constant setting = 4, and thus, only this segment of data will be used for comparison between the control pile and the test pile.

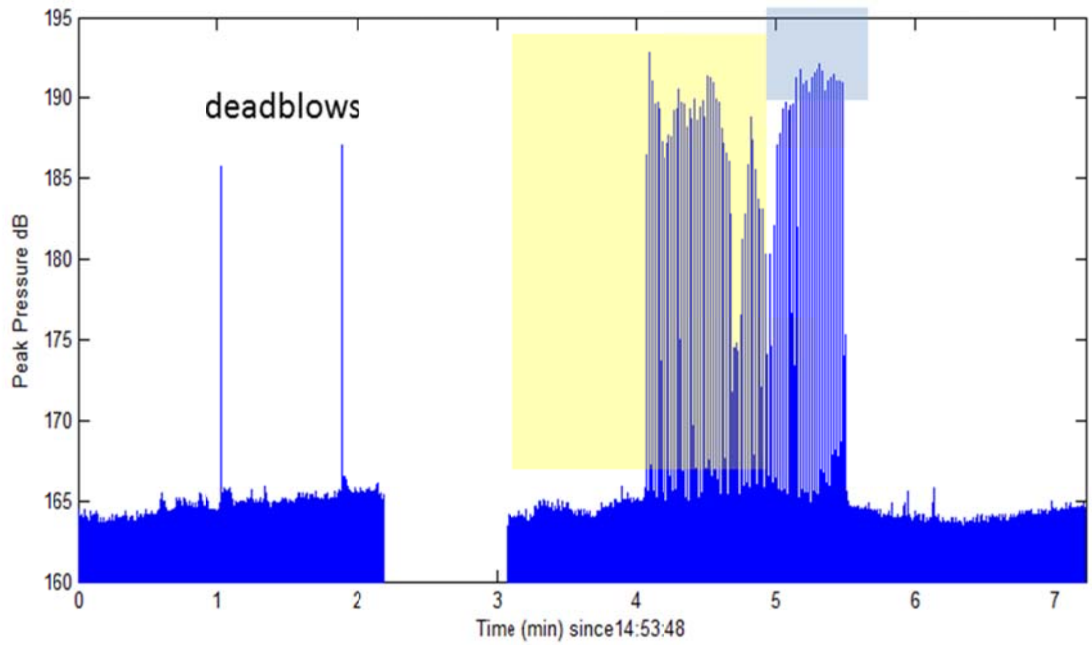

Figure 12. Pressure recording from channel 9 (lowest channel) of the VLA showing all hammer strikes made during double wall pile test on October 29th. (No strikes occurred during the period between approximately 2 and 3 min.) Starting at approximately minute 4 on this scale fuel settings were changed in an unknown manner and duration causing the modulation shown in yellow shade. The blue shade denotes the period where fuel setting was definitively set to, and held at constant setting = 4. NOTE: pressure is absolute pressure expressed in dB re 1 μPa.

For measurement phase 3 on October 30th involving the mandrel test pile commencing approximately 09:16 pm, the basic sequence was as follows:

(i) Three "deadblows" defined as impacting the pile with weight of the hammer only, without additional energy supplied to the hammer.

(ii) A series of strikes during which the hammer fuel setting was changed from 1 to 4 (involving settings 1-2-3-4). No bubble curtain was involved. This series started about 1 min after the deadblows.

(iii) A final series of strikes during which hammer fuel setting was at maximum = 4. This series started about 2 min. after completion of with sequence (ii)

The complete record involving the double wall test pile is shown in Fig. 13. Note in this case we have chosen to show the record as measured at the remote site located 135 m from the pile. The same situation as regards to meta data exists on October 30th, and the changes made during the period denoted by the yellow shade cannot as yet be further interpreted. The blue shade denotes the period where fuel setting was definitively set to, and held at constant setting = 4. Thus, data from three deadblows, and the blue shaded area will be used for comparison between the control pile and the mandrel test pile.

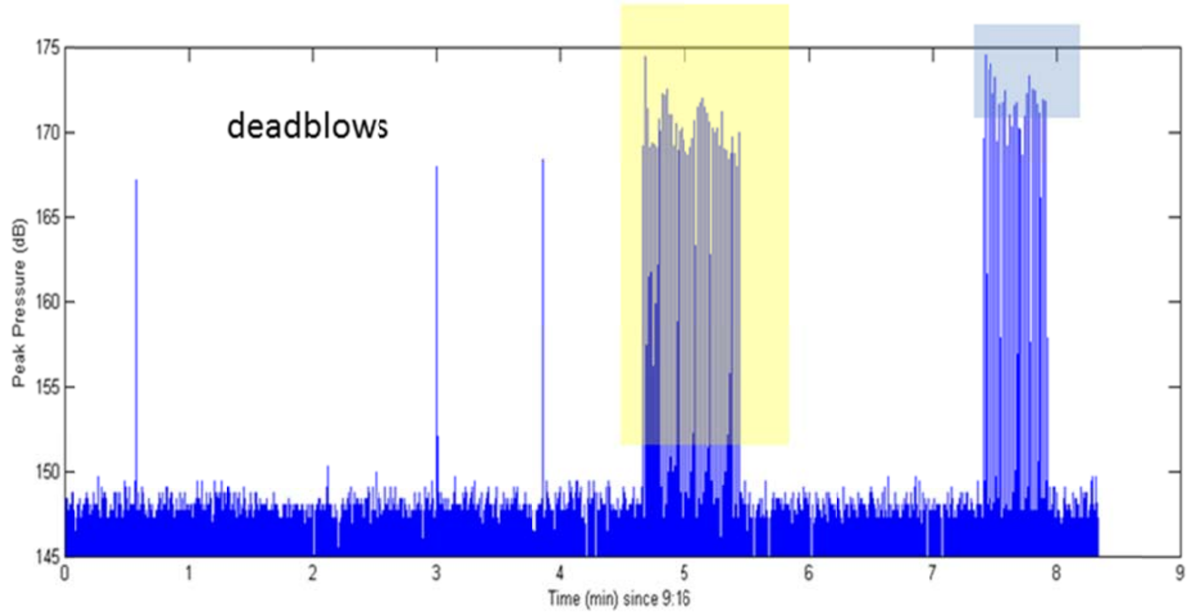

Figure 13. Pressure recording from the autonomous system at range 135 m on all hammer strikes made during mandrel wall pile test on October 30th. Starting at approximately minute 4.5 on this scale fuel settings were changed in an unknown manner and duration causing the modulation shown in yellow shade. The blue shade denotes the period where fuel setting was definitively set to and held at constant setting = 4. NOTE: pressure is absolute pressure expressed in dB re 1 μPa.

V. Comparisons between the Control and the Test Piles

Comparisons at the Vertical Line Array (VLA)

Three sound metrics are computed from the acoustic measurements for use in comparing the sound fields originating from the control pile and the two test piles. The first is the peak pressure defined as the maximum absolute value of the pressure for a given strike, expressed in dB re 1 μPa. For example, Figs. 10-13 show some "quick look" estimates of this metric.

The remaining two are Sound Exposure Level (SEL) and RMS pressure, defined over the time span corresponding to 90% of the energy of the received pulse as shown in by the red segment in Fig. 14. The RMS pressure and SEL are simply related by the 90% energy time span, and an operation as shown in Fig. 14 is done on every pressure time series associated with pile strike, received on each hydrophone.

Figure 15 examples of PEAK, RMS and SEL as measured on channels 1 and 9 on the VLA, from control pile (left column) and the double wall test pile (right column); these channels chosen to give a representative picture of the shallowest (channel 1) and deepest (channel 9) measurement. The shaded areas in each case denote the section of steady conditions during which the hammer fuel setting equaled 4, and over which averages are made of the metrics comparison. For example, the blue shaded area for the double wall test pile corresponds to the blue shaded area in Fig. 12.

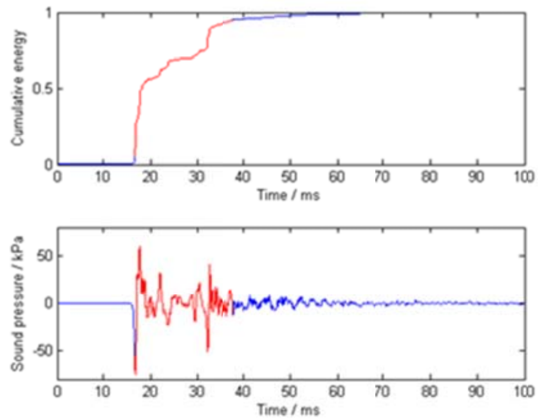

$$\mathrm{SEL}_{90} = 10\log_{10}\left(\int_{T_5}^{T_{95}} \frac{p(t)^2}{p_{\mathrm{ref}}{}^2 t_{\mathrm{ref}}}\,\mathrm{d}t\right)$$

Figure 14. Illustrating the definition of the time span corresponding to 90% of the energy of a broad band pulse. The time span, red segment in lower left figure is determined by squaring and integrating the pulse in a cumulative sense (upper left figure) after which the 0.05 –to- 0.95 energy time duration is determined. SEL is then computed over this time duration as shown in right panel.

The key results from the testing on October 29th as measured at the VLA site are shown in Fig. 16. The legend identifies the three metrics with color code. The metrics as a function of depth for individual strikes are shown by thinner lines of the same color, with results from control pile (CP) distinguished from the double wall test pile (DW) by the solid and dashed thick lines, respectively, used to represent the *linear average* (i.e, non-decibel average) of the strike data expressed in decibels.

Note that depths for the CP and DW cases differ for the October 29th owing to the 0.9 m tidal difference between about 1 pm (CP) and 3 pm (DW). The individual strike data from the CP and DW are not comparable, however, the linear averages are comparable. The difference in dB between the CP and DW for each hydrophone, i.e., comparing hydrophone 1 with 1, 9 with 9, etc., is shown by the three columns of 9 numbers each representing in order left to right: SEL, RMS and PEAK.

Of the three metrics, PEAK will typically have the highest variance because it is literally based on one time sample. In contrast, SEL is the most robust measure because of its time-integration property. In terms of the individual strike data we generally observe a higher degree fluctuation in the PEAK data (red) and lower fluctuation in SEL data (blue).

The row of larger numbers at the bottom of the plot is as follows: for RMS and PEAK these numbers are the average of the column of decibel-numbers directly above which are associated with each channel. A true depth-average of PEAK is somewhat ill-defined, and this is also the case for RMS for a transient pulse. However the average values as we have computed them do represent the central tendency of the noise reduction for these metrics.

For SEL the number (17.2 dB) represents the decibel difference of the sum of time integrated squared pressures (Fig. 14), over all channels. This is the most robust estimate of noise reduction as it attempts to capture all the noise energy at least over the 5.6 m span of the VLA.

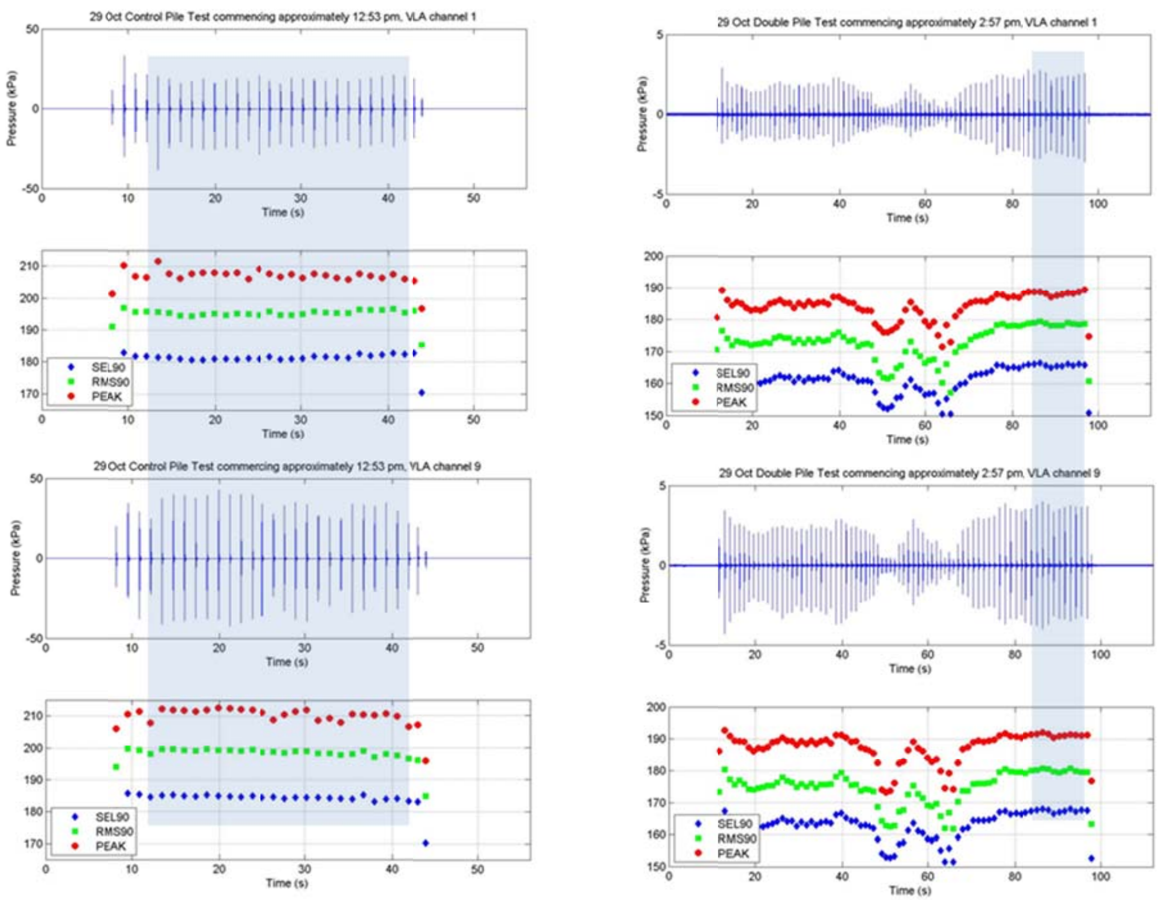

Figure 15. Channels 1 and 9 of the VLA corresponding to the October 29th series of test, with control pile data shown in left column and double wall test pile data shown in right column. The shaded areas in each case denote the section of steady conditions during which the hammer fuel setting equaled 4, and over which averages are made of Peak Pressure, SEL and RMS pressure, for comparison. For example, the blue shaded area for the double wall test pile corresponds to the blue shaded area in Fig. 12. Note the differing time scales that reflect the last sequence of strikes for the control pile and a longer sequence of strikes for the double wall pile with this sequence ending with fuel setting 4.

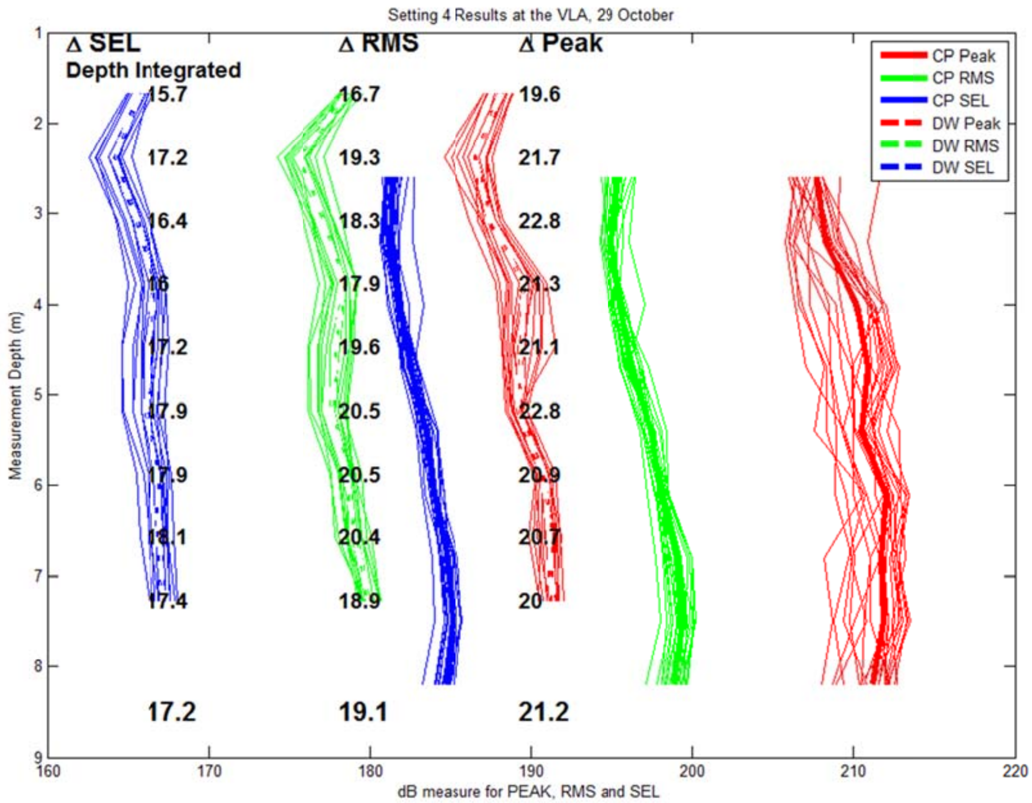

Figure 16. Key results of the fuel-setting-4 tests made on the control pile (CP) and double wall (DW) test pile on October 29th as measured at the VLA. Legend identifies the three metrics and color code with thicker solid line (CP) or dashed line (DW) showing the linear average over the strikes. Individual strike data shown by thinner lines of same color (in some cases hidden by thicker line). The three columns of numbers correspond to the decibel difference in mean value for the 9 hydrophones, with columns going from left to right representing SEL, RMS and PEAK. Bottom row of larger numbers is the depth average of each column for PEAK and RMS. For SEL the bottom number is the difference in depth integrated SEL as discussed in the text.

The VLA results from October 30th testing involving the Mandrel pile are shown in Figs. 17 and 18. As with the double wall test pile, results in terms of estimating noise reduction are compared with the control pile measurements made on October 29th. Figure 17 shows as sample of the strikes measured at the VLA during fuel-setting-4 and Fig. 18 is completely analogous to Fig. 16.

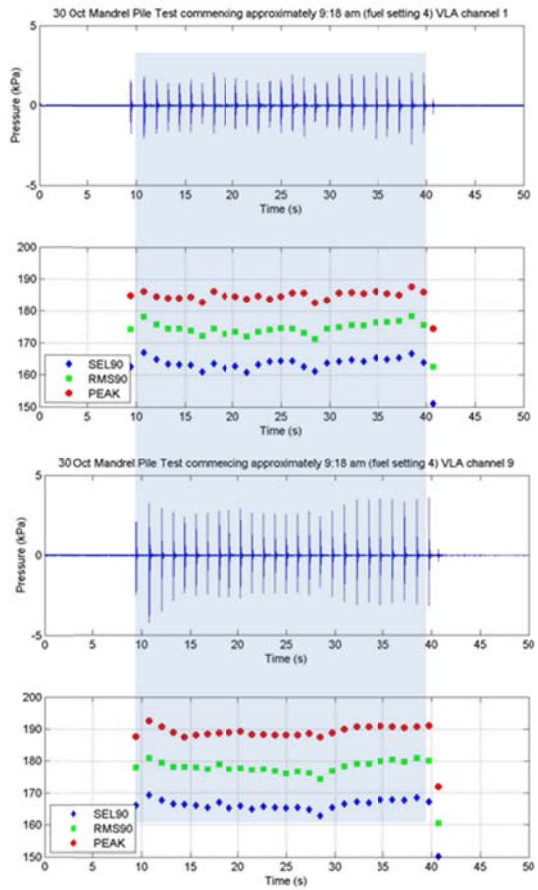

Figure 17. Channels 1 and 9 of the VLA corresponding to the October 30th series of tests involving the mandrel pile. This data is compared with control pile data shown in left column of Fig. 15. Data from shaded areas used in the comparison.

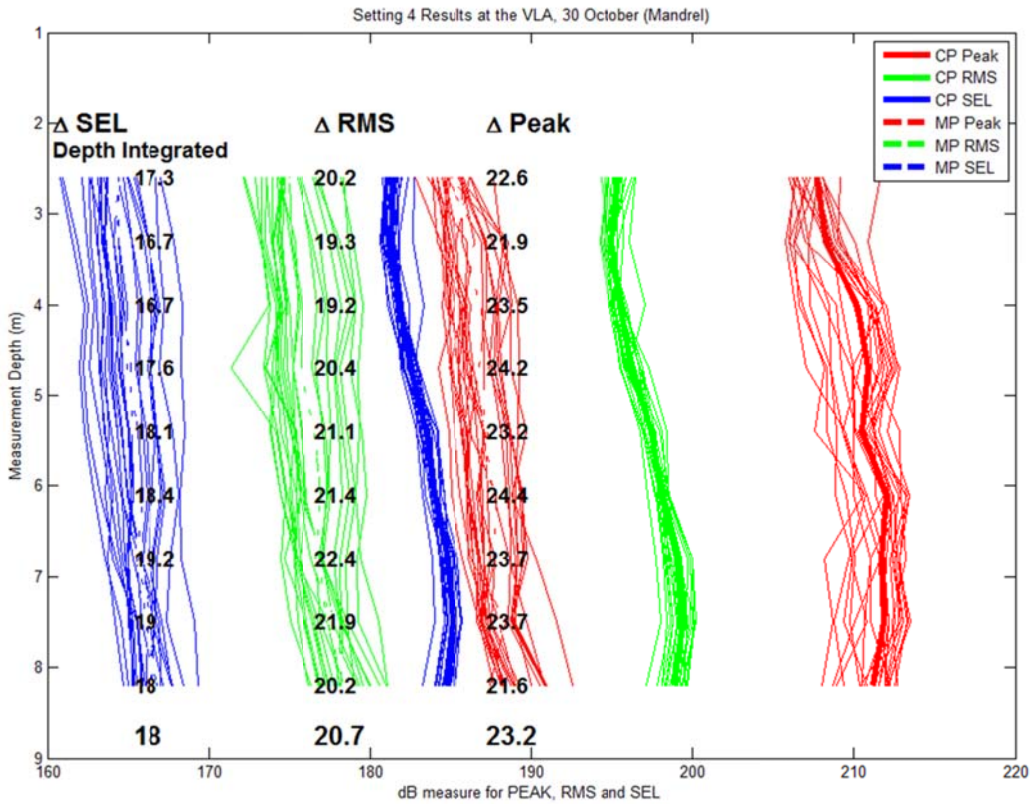

Figure 18. Key results of the fuel-setting-4 tests made on the control pile (CP) and Mandrel test pile (MP) on October 30th as measured at the VLA. Legend identifies the three metrics and color code with thicker solid line (CP) or dashed line (MP) showing the linear average over the strikes. Individual strike data shown by thinner lines of same color (in some cases hidden by thicker line). The three columns of numbers correspond to the decibel difference in mean value for the 9 hydrophones, with columns going from left to right representing SEL, RMS and PEAK. Bottom row of larger numbers is the depth average of each column for PEAK and RMS. For SEL the bottom number is the difference in depth integrated SEL as discussed in the text.

For continuing to the remote measurements it is worthwhile to revisit the two SEL reduction numbers 17.2 dB for the DW and 18.0 dB for the MP. The SEL data from the VLA test are shown below in Fig. 19 where now the horizontal axis is simply hydrophone number. As in Figs. 16 and 18, fluctuations in the individual strikes is evident (though less than the RMS and PEAK metrics). Reasons for the slightly greater degree of fluctuation for the MP tests are possibly associated with leakage in a seal that allowed water to enter the space between the two piles. However both DW and MP settle into similar linear averages over the strikes (black squares.) These averaged data are then summed (in linear space) over the 9 hydrophones to represent a kind of depth-integrated SEL, with the decibel differences shown.

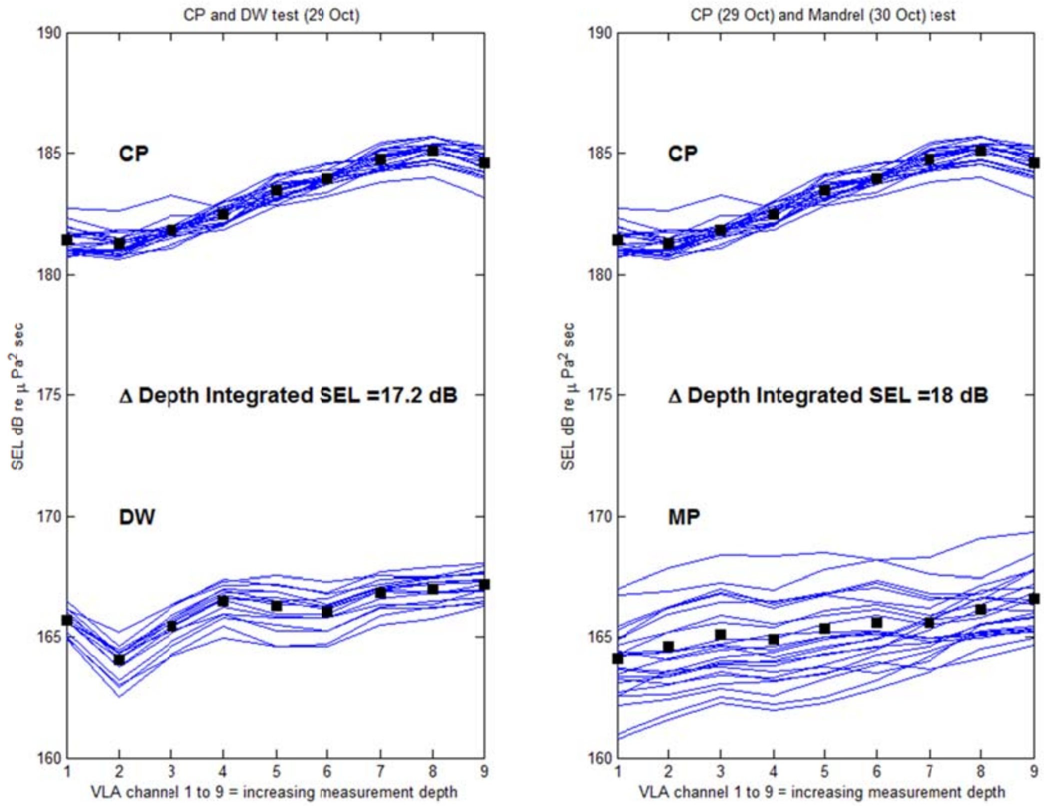

Figure 19. SEL as a function of hydrophone channel for individual strikes (thin blue lines) for the control pile (CP), double wall test pile (DW) and mandrel test pile (MP). Black squares denote the linear average of individual strike SEL for each hydrophone. These data are then summed over all hydrophones (in linear space) with the result decibel difference shown for each test (17. 2 dB for the DW test, and 18 dB for the MP test.

Comparisons at the two remote sites

The results from October 29th testing as measured at the two remote sites are shown in Fig. 20, and from the October 30th testing in Fig. 21.

Here the legend color code also identifies the three metrics. Individual strike data is indicated by asterisks and these correspond one-to-one with those measured at the VLA. The linear averages of the strike data are shown by the closed squares for the control pile (CP) on October 29th, and open squares for the double wall pile (DW) and mandrel pile (MP).

The rows of numbers are the decibel difference in mean values going from left to right: SEL, RMS and Peak, which are measured at range, 122 m (lower row) and 502 m (upper row) for October 29th, and ranges 135 m and 517 m for October 30th.

We observe that the 17.2 dB value for difference in depth integrated SEL at the VLA has reduced to ~14 dB at range 122 m, then increased back to at more consistent 16 dB at range 502 m. The mandrel pile test results, although necessarily compared with control pile test from the day before, are very similar to the double wall pile results insofar as we also observe a ~14 dB at range 135 m, which then increased back to at more consistent 16 dB at range 517 m.

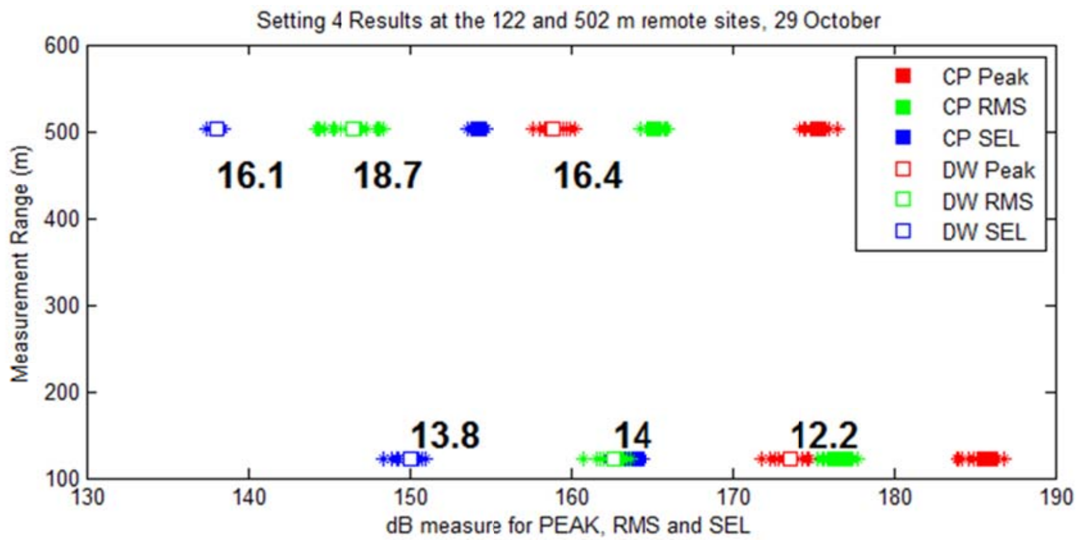

Figure 20. Key results of the fuel-setting-4 tests made on the control pile (CP) and double wall (DW) test pile on October 29th at the two remote sites, range 122 m (1.4 m off the bottom) and range 502 m (10 m measurement depth). Legend identifies the three metrics with closed squares (CP) or open squares (DW) showing the linear average over the strikes. Individual strike data shown by asterisks and which correspond one-to-one with those measured at the VLA. The rows of numbers correspond to the decibel difference in mean values going from left to right: SEL, RMS and Peak, measured at range, 122 m (lower row) and 502 m (upper row).

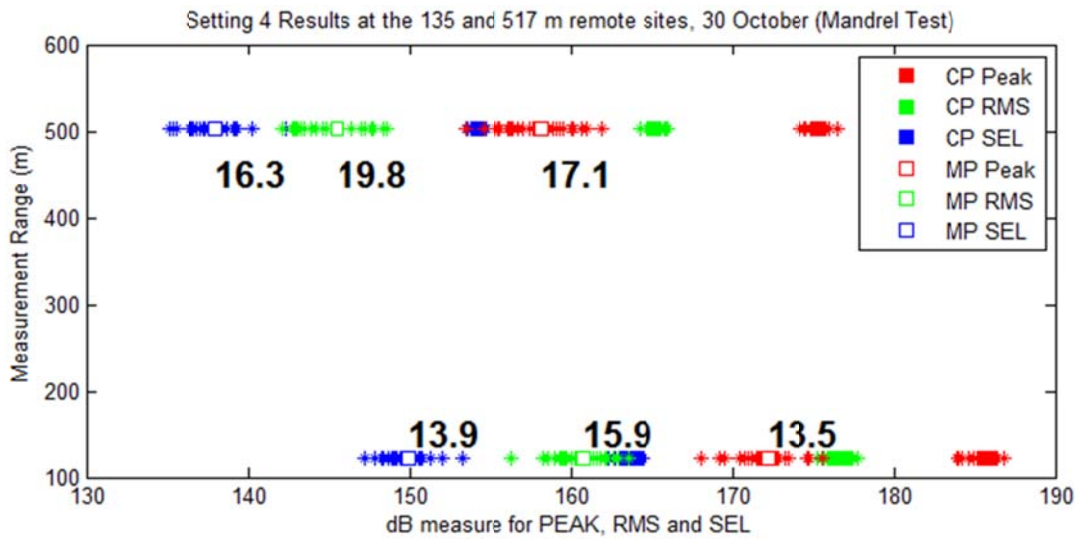

Figure 21. Key results of the fuel-setting-4 tests made on the control pile (CP) and Mandrel test at the two remote sites, range 135m (1.4 m off the bottom) and range 517 m (10 m measurement depth). Legend identifies the three metrics with closed squares (CP) or open squares (MP) showing the linear average over the strikes. Individual strike data shown by asterisks and which correspond one-to-one with those measured at the VLA. The rows of numbers correspond to the decibel difference in mean values going from left to right: SEL, RMS and Peak, measured at range, 135 m (lower row) and 517 m (upper row).

VI. Summary of Underwater Noise Attenuation Results

Table 1 below summarizes the results for underwater noise reduction performance for the SEL, RMS and Peak pressure metrics, for the double wall test pile measured on October 29th (yellow shade) and mandrel test pile measured on October 30th (green shade), where in both cases the reduction is relative to the control pile measurements made on October 29th.

At first glance it may seem curious that for a given metric the performance depends on the range measured. For example, for the double wall test pile measurement made on October 29th, SEL reduction was 17-18 dB at the VLA, decreased to ~14 dB at the 122 m and 135 m sites, and then increased to 16 dB at the 502 m and 535 m sites.

Measurement Range	VLA: 8-8.5 m		Remote 1: 122-135 m		Remote 2: 502-535 m	
SEL Reduction (dB)	17.2	18.0	13.8	13.9	16.1	16.3
RMS Reduction (dB)	19.1	20.7	14.0	15.9	18.7	19.8
PEAK Reduction (dB)	21.2	23.2	12.0	13.5	16.4	17.1

Table 1. Summary of noise reduction in decibels for the SEL, RMS and peak pressure metrics. Yellow shaded values are for double wall test pile (Oct 29th test), and green shaded values are the mandrel pile (Oct 30th test). Slightly different ranges apply to the remote measurements made on October 29th and 30th.

However, the field from impact pile driving is complex and spatially varying. Figure 22 shows a notional field strength of a metric proportional to SEL from impact pile driving, along with the approximate bathymetry for the Tacoma site, and locations of the VLA and two remote measurements. The field is produced using the parabolic wave equation and implementing the phased Mach-wave approach outlined in Reinhall and Dahl[1]. An important characteristic of this field is the spatially-varying field seen reflecting from the surface and bottom and adjusting to the increasing depth. It is anticipated that the acoustic field from a noise-suppressed pile will have less of this characteristic.

Therefore, at some remote measurement locations it is possible to measure a reduced level of sound from impact pile driving, in comparison with the level associated with that from a noise-suppressed pile. Such a location might be in the vicinity of 700 m at depth 10 m, which is one reason we avoided this range. This might have also influenced the measurements at range 122 m (and 135 m).

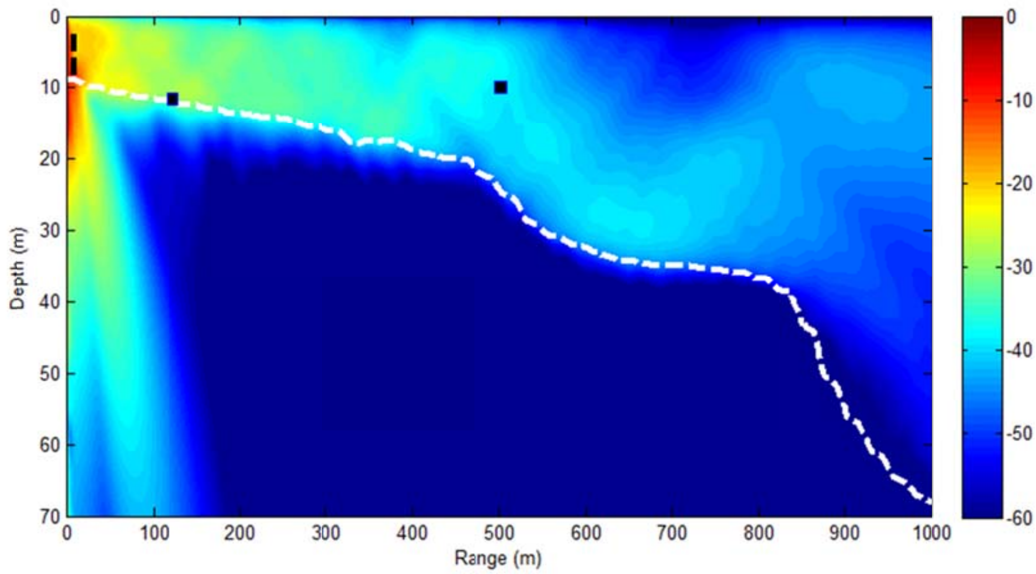

Figure 22. Notional field strength in decibels for SEL (i.e., proportional to) from impact pile driving based approximately bathymetry (white dashed line) for the Tacoma site and tidal conditions in effect at 1300 on October 29th. The black marks show approximate locations of the vertical line array near range 8 m, and the two remote measurements at ranges 122 m and 502 m.

Appendix A: Spectral Content of Sound Exposure Level (SEL)

Figure A1 shows the Sound Exposure Level (SEL) as a function of frequency for measurements made on the VLA (channel 9). The results indicate that the reduction of SEL measured for the two test cases occurred over a broad range of frequencies without necessarily being frequency selective.

[1] Reinhall, P.G. and P. H. Dahl, "Underwater Mach wave radiation from impact pile driving: Theory and observation', J. Acoust. Soc. Am., 130, Sep. 2011, pp. 1206-1216.

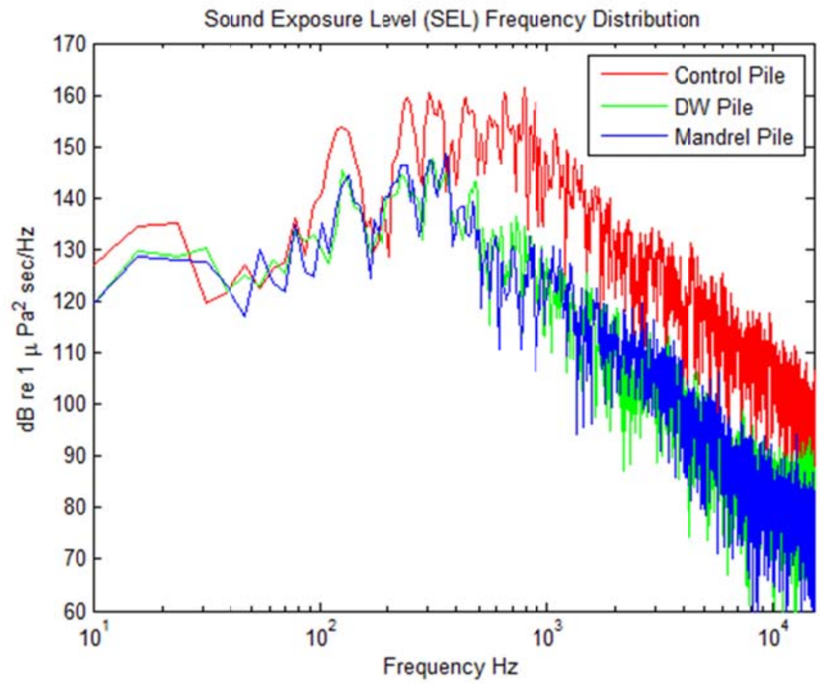

Figure A1. Frequency distribution of SEL for the Control Pile and two test piles.

Appendix B: Cumulative SEL (cSEL) for October 29th and October 30th

On October 29th there was a total of 185 strikes made as part of the Control Pile and the Double Wall Pile testing . At the remote range of 122 m the cSEL is 183 dB re 1 μPa^2 sec, based on computation of the single SELs for all the strikes shown below in Fig. B1. Therefore, the 187 dB cSEL isopleth radius was less than 122 m on October 29th. Based on the modeling shown in Fig. 22 we estimate the range to the 187 dB cSEL isopleth as approximately 60 m.

On October 30th, there was a total of 70 strikes involving the Mandrel pile, which put the cSEL at 168.3 dB re 1 μPa^2 sec at the 135 m remote measurement range. At the VLA site, the typical single SEL on channel 9 was 166 dB (see Fig. 18). Assuming this value applied to all 70 strikes, this puts the cSEL at 184 dB re 1 μPa^2 sec at the VLA range of about 8 m. Therefore the 187 dB cSEL isopleth radius was less than 10 m on October 30th.

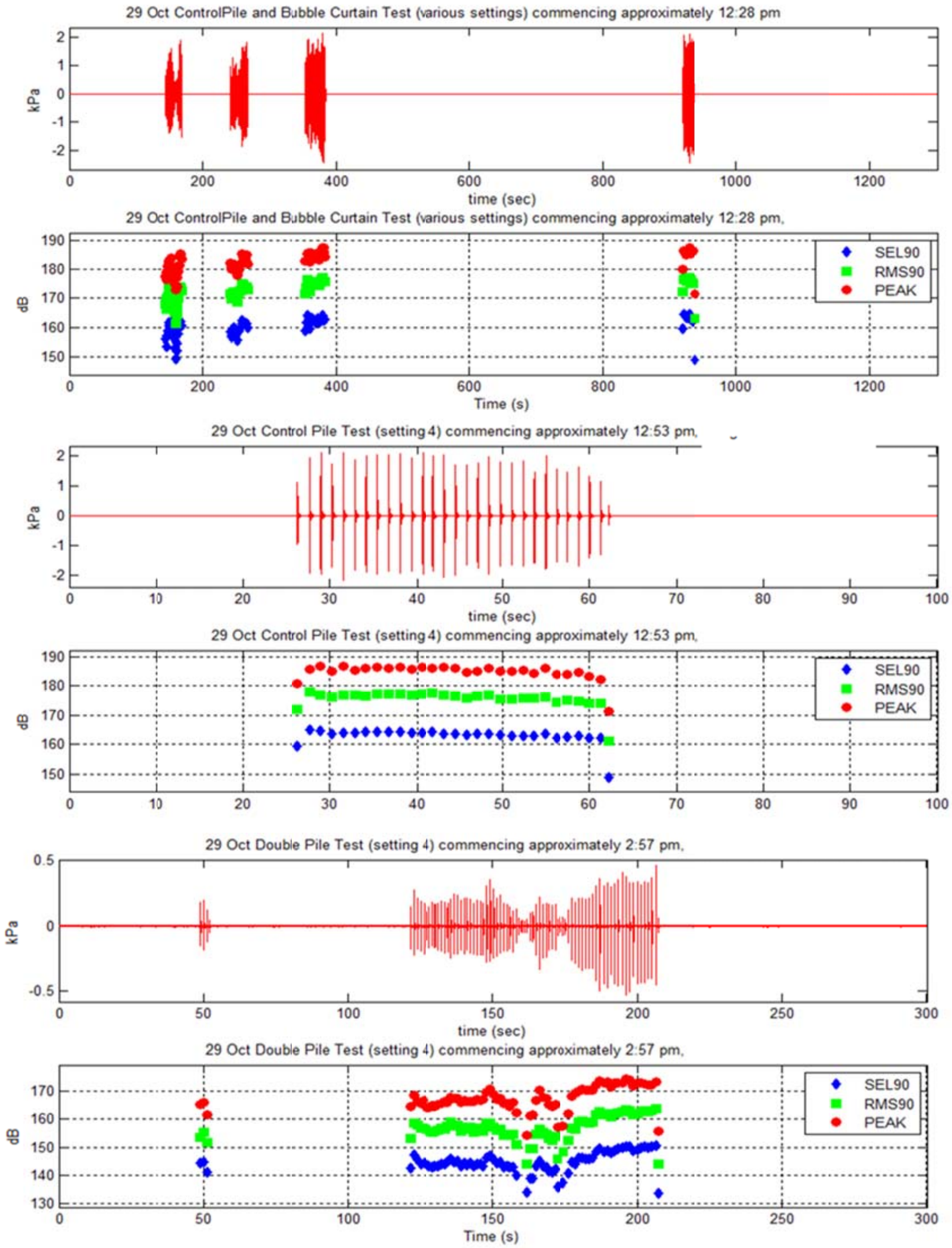

Figure B1. History of all 185 strikes made on October 29th as measured at range 122 m.